Report on Deliverable

Project	H2020 - SURE (Grant-Number 654662)
Deliverable	**D7.5 – Comparison of RJD reservoir performance to conventional wells**
Work package	WP7 - Integration
Lead author	Elisabeth Peters (TNO)
Contributors	Guido Blöcher (GFZ), Rohith Nair (TNO), Kees Geel (TNO), Saeed Salimzadeh (DTU)
Dissemination level	PU (public)
Type	R (document, report)
Due date	2019-02-28
Actual submission date	2019-06-03
Resubmission date(s)	

Licence information	Report D7.5 of the Consortium of the H2020 SURE Project This publication is licensed under a Creative Commons License, International Attribution 4.0: CC BY
DOI (Repository)	10.2312/GFZ.4.8.2019.010
Recommended Citation	Peters, E., Blöcher, G., Nair, R., Geel, K., Salimzadeh, S.; The Horizon 2020 Project SURE: Deliverable 7.5 - Comparison of RJD reservoir performance to conventional wells, 2019, Potsdam: GFZ German Research Centre for Geosciences, DOI: 10.2312/GFZ.4.8.2019.010

Table of Contents

DOI: 10.2312/GFZ.4.8.2019.010

1. Executive Summary

Radial Jet Drilling (RJD) is a technique to stimulate wells by creating small-diameter laterals from vertical or deviated wells using hydraulic jets. The laterals, also called radials, can be up to 100 m in length. To analyze under which sub-surface conditions the radials improve the well performance most, a step-wise approach is followed in which first the performance of a single stimulated well is analyzed and in a second step, the performance of a doublet system is analyzed. Finally, case studies that are more detailed are simulated.

For the single well case, a good first estimate of radial stimulation performance for different reservoir conditions can be obtained from (semi-) analytical solutions. These results show that the anisotropy in the permeability and the thickness of the reservoir influence the *relative* increase in productivity/injectivity most. The permeability influences in particular the *absolute* performance of the stimulated well. Many aspects not included in the semi-analytical solution also influence the performance of the radial stimulation:

- Since the radials are open hole, stability for friable rocks or deep reservoirs is unlikely. This depends on the in-situ stress conditions. Collapsed radials probably have much lower performance or no effect at all.
- The uncertainty in the radial path and diameter decreases the expected benefits from radials significantly depending on the type of reservoir. For example for a layered reservoir, the expected increase may be tens of percent lower.
- Due to the small diameter (0.02-0.05 m) and rough surface of the radials and the high rates of geothermal wells, viscous pressure drop due to flow in the radials has to be taken into account for prediction of performance. For example for a radius of 0.04 m and well rate of 3600 m^3/d, expected increase in performance is halved when taking into account pressure drop.
- Heterogeneity in the permeability has a strong impact on the performance of the radials. Performance of individual radials depends in first approximation on the local permeability. However, this is difficult to capture in general terms.
- Near well bore damage (positive skin) and prior stimulation (negative skin) have a large impact on the expected increase due to stimulation. In case the radials can be used to by-pass near well damage, performance can be much higher than predicted using the analytical equations.
- Heterogeneity due to fault and/or fractures, voids, sharp transitions or layering all make potential success more uncertain and predictability lower due to potential issues with jetting.

Whether increased performance for a single well can be translated to similar increased performance of a doublet depends on the doublet settings and subsurface conditions. For a fixed doublet distance or field size, an increase in rate due to improved performance of the wells will result in a reduced field life. The increased well performance can also be used to lower pumping cost at a fixed rate and thus improve performance of the doublet. It was found, that for most subsurface systems, the impact of the radials on production temperature was minor (for constant rate). Only for some fractured systems, short-circuiting can be increased due to radials. Overall, the ideal candidate for radial stimulation is a reservoir which is not too deep, in homogeneous, competent rock with a well with near well bore damage or in a not too deep anisotropic reservoir in which the main well is not drilled beneficially compared to the main direction of permeability.

GFZ German Research Centre for Geosciences
DOI: 10.2312/GFZ.4.8.2019.010

2. Introduction

To economically produce a geothermal resource, wells with sufficient productivity are a key element. However, for a variety of reasons well productivity can be lower than expected or decline over time, for example because of disappointing reservoir transmissivity or because of well problems, such as scaling or near well bore damage. One of the options to enhance the productivity of a well are small-diameter laterals. For bypassing a skin such a lateral need not be very long (up to 10 m should be enough), but for connecting the reservoir better to the well in case of e.g. low permeability, longer laterals are a better choice. A technique which can achieve a distance of up to 100 m is radial jet drilling (RJD) (Kamel et al., 2017; Yan et al., 2018). Laterals created using this technique are also referred to as radials. The original well in which the laterals are jetted is also referred to as the backbone. The technique has been developed in the petroleum industry and is relatively new for geothermal applications and still under development. One of the limitations is that the jets cannot be steered and thus the realized path is uncertain (Reinsch et al., 2018).

RJD is not applicable in all reservoir rock types or under all conditions. In general, the limitations that are mentioned for current application of RJD are those as listed in (Abdel-Ghany et al. 2011) (e.g. Ragab, 2013; Blöcher et al., 2016; Kamel, 2017; Ibeh et al., 2017), which include limitations on temperature and depth of the application. These limitations are mostly related to limitations of the equipment and well completions and not necessarily to limitations of the process as relating to the formation. The main limitation related to the formation is porosity which should be higher than 3-4 %. Protim Maut and co-workers (2017) present a more detailed list of reservoir factors and well characteristics to be considered before implementing a successful RJD job. Mostly, variations in lithology (e.g. porosity), steeply dipping formations and unconformities are mentioned as disqualifiers for a successful job. Also reservoirs with near zero porosity, evaporates (salt, gypsum, anhydrites) and unconsolidated formations are listed as unsuitable for jetting. Jun et al., (2018) mention that it is difficult to jet formations with high mechanical strength and that porosity should be higher than 5% for coal formations and higher than 10 % for oil bearing formations. Also permeability is mentioned as a constraint (> 1 mD). Several authors mention that friable and/or unconsolidated formations should be avoided (Bruni et al., 2007; Abdel-Ghani et al., 2011; Ragab, 2013; Protim-Maut et al., 2017).

From published field cases, it is not clear in which type of reservoir rocks and ambient conditions the best results have been obtained so far (Blöcher et al., 2016). Most published field cases are in sedimentary rocks: mostly sandstone/siltstone and some limestone (Cinelli and Kamel, 2013) or carbonate (Elliott, 2011; Yan et al., 2018). The following documented cases were found:

- Golfo San Jorge Basin and Neuquen Basin in Argentina (Bruni et al, 2007)
- Belayim field, Egypt, sandstone (Abdel-Ghany et al., 2011; Ragab, 2013)
- Urtabulak field, Uzbekistan, carbonate (Elliott, 2011)
- K-block, Tarim field China (Teng et al, 2014)
- The Donelson West Field, USA, limestone (Cinelli and Kamel, 2013; Kamel, 2014)
- Siltstone, China (Wang et al., 2016)
- Klaipėda, Lithuania, layered sandstone, geothermal application (Blöcher et al., 2016)
- Assam Arakan basin, sandstone (silty, with shales) (Protim-Maut et al., 2017)
- Mature oil field in North Kuwait with layered sandstone (Al-Jasmi et al., 2018)
- Carbonate reservoir, China (Yan et al., 2018).

DOI: 10.2312/GFZ.4.8.2019.010

Peters et al., (2015) conclude from an analysis of published case studies that results are highly variable and that best results appear to be achieved in case of near-well damage (positive skin). Kamel et al. (2017) conclude from an analysis of three case studies that candidate selection, including in-situ stress analysis and rock mechanics is an essential part of the analysis, however no publications have been found to date that discuss the impact of ambient conditions such as depth and in-situ stress conditions on the results of an RJD job for field cases. Hahn et al. (2019) present results of jetting experiments under reservoir conditions, which provides information on jettability under reservoir conditions, but not on the subsequent performance. Also several simulations studies analyse the performance of radials in different cases (Abdel-Ghany et al., 2011; Balch, 2014; Peters, 2015; Peters et al., 2015; Maaijwee, 2018) of which the last two are for geothermal systems. Due to differences in the approaches and assumptions, results vary and are not straightforward to interpret.

The goal of the research described in this publication is to identify the subsurface conditions (in terms of reservoir rock type and ambient conditions) which are most favourable for increasing well performance by stimulation with RJD. The focus is on sedimentary rock, both sandstone and limestone/carbonates, because these rock types are most likely to be jettable. Jettability of the rock is not taken into account explicitly in this analysis, because here we investigate the potential of the radial geometry. The impact of the well completions on RJD application is not included in this analysis. The type of conditions of interest are reservoir rock type characterised by for example permeability (possible anisotropy, fracture versus matrix, heterogeneity), porosity and rock strength and ambient conditions such as stress regime, depth and temperature. The reservoir rock characteristics and ambient conditions influence both the result of the radial jet drilling (in terms of length, diameter, stability and orientation of the laterals) and the impact of the stimulation with radials (in terms of increase in heat production). Since this means an extremely large range of possible combinations, explicit simulation taking into account all relevant physical processes and radial well designs is essentially impossible. Therefore a different approach is followed.

The approach chosen to identify favourable conditions for jetting is stepwise: first an overview is created for a broad range of conditions with many simplifying assumptions. In the next step, these conditions are relaxed to evaluate their impact. In the last step, a number of case studies is evaluated in which different aspects are combined to form a complete picture. In more detail, the steps are as follows.

1. The first step is to analyse the change in injectivity/productivity due to radial stimulation of a single well in an infinite reservoir. Semi-analytical solutions are used to analyse a wide range of the following rock characteristics: permeability, reservoir height and anisotropy in the permeability. Main assumptions taken to derive the analytical solutions are: homogenous properties, straight laterals with constant diameter, laterals are always stable and no pressure drop due to flow in the laterals.
2. In the second step the impact of the various assumptions in the first step is analysed. A distinction is made between factors impacting the injectivity/productivity of an individual well and the impact on the performance of a geothermal system (doublet) as a whole. The latter is mostly the impact on cold water breakthrough and of limited field size.
3. Finally, example simulation cases of a doublet are discussed in detail.

DOI: 10.2312/GFZ.4.8.2019.010

Both single and dual permeability reservoirs are investigated. The numerical methods used for the simulations have been validated by comparison with analytical solutions where possible and otherwise by comparison with different methods (Peters et al., 2018 and 2019).

In Chapter 3, the changes in productivity/injectivity of a single well are described. In Chapter 4, the effect of RJD stimulation on the geothermal system as a whole is investigated. In these chapters also the previously published simulation results are discussed. In Chapter 5, detailed case studies are presented. Summary and conclusions are in Chapter 6.

DOI: 10.2312/GFZ.4.8.2019.010

3. Single well Injectivity/productivity

3.1 Homogeneous case

A good, first approximation of the improvement achieved by adding radials on injectivity/productivity can be derived from (semi-)analytical solutions. (Semi-)analytical solutions assume homogeneous reservoir properties, such as permeability and porosity and simple reservoir geometry, but allow for fast approximation of the increase due to laterals. Peters et al (2015) have used a semi-analytical tool to analyse the increase due to radial stimulation for a variety of input parameters. They have shown that the main reservoir parameters that have impact on the relative radial contribution are the anisotropy in the permeability and the thickness of the reservoir (Figure 3-1). Figure 3-1 shows the Productivity Increase Factor (productivity of stimulated well / productivity of the unstimulated well (PIF)) as a function of the anisotropy in the permeability and height of the reservoir for stimulation of a vertical well with 8 radials (distributed over 4 kick-off depths). The anisotropy is important because it determines the distribution over vertical versus horizontal parts of the well: for high vertical permeability (sub-)horizontal are more beneficial. For thickness of the reservoir they showed decreasing impact of the same number of laterals for a thicker reservoir. The permeability as such did not impact the *relative* increase resulting from the radials under the assumptions of that study. The *absolute* increase in production did increase with increasing permeability.

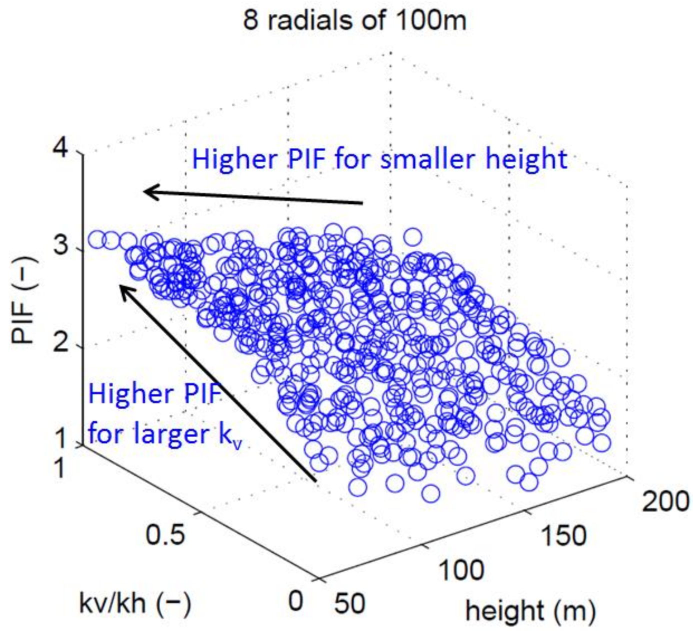

Figure 3-1. Illustration of the main conclusions showing the increase in PIF (productivity of stimulated well / productivity of the unstimulated well) as a function of anisotropy and reservoir height for 500 samples. (reproduced from Peters et al., 2015)

The increase due to the laterals was quite linear with the total length of laterals jetted (calculated by summing the length of all laterals) (Figure 3-2). Although longer laterals are better than the same length of laterals divided over shorter laterals (Figure 3-2, compare 4 radials of 50 m with 8 radials of 50 m). The productivity increase can also be represented by a skin: for example stimulation with 8 radials of 100 m can also be represented by a skin of -5.2.

DOI: 10.2312/GFZ.4.8.2019.010

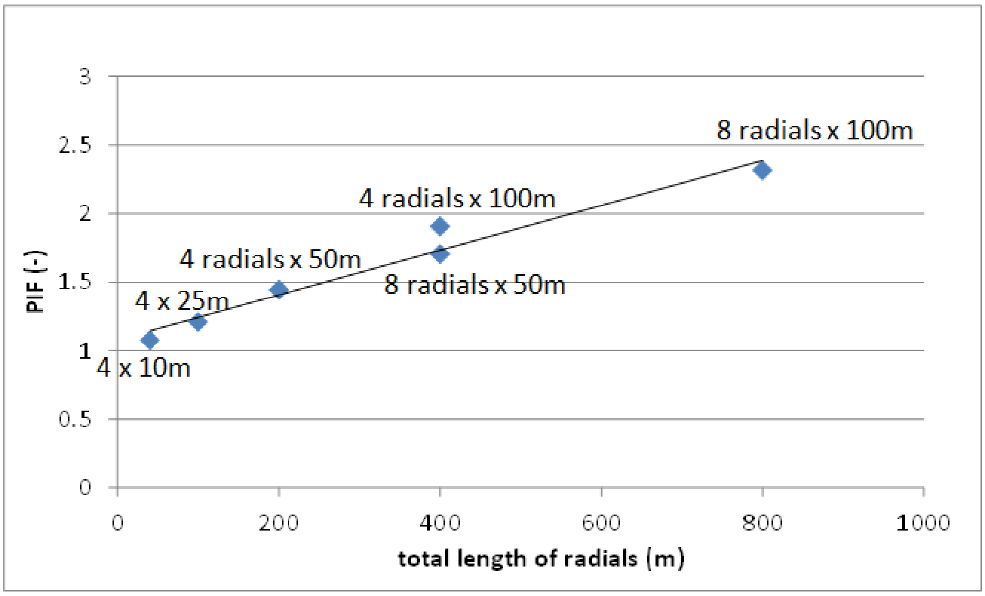

Figure 3-2. Mean PIF (productivity of the (stimulated) radial well / productivity of the unstimulated well) from 500 samples as a function of the total length of radials jetted (reproduced from Peters et al., 2015).

The main assumptions of the analysis are:

1. Homogeneous properties
2. Straight laterals without uncertainty in the lateral path.
3. No pressure drop in the wells/laterals
4. No skin
5. Laterals are stable with a circular hole with constant diameter.
6. Single well analysis
7. Infinite reservoir

The first five points affect the productivity/injectivity of a well. In the following, each of these assumptions will be relaxed in turn to understand its impact on the performance of stimulation with laterals. The last two points are relevant for the long-term impact of laterals and will be discussed in Chapter 4.

3.2 Heterogeneous properties

The impact of heterogeneity in reservoir properties is difficult to analyse generically. Peters et al. (2016) studied the effect of heterogeneous permeability in horizontal direction by generating Gaussian random fields to represent permeability. The settings were based on an existing geothermal field. They concluded that on average the behaviour of the radials was the same as for homogeneous systems. Results of individual realisations depended strongly on the permeability along the radial paths. Adding more radials also reduces the difference between individual reservoirs, because more of the reservoir is sampled. So having more radials can be seen as a way to reduce risk in some cases.

DOI: 10.2312/GFZ.4.8.2019.010

For vertical heterogeneity (layered reservoirs), the uncertainty in the lateral path can have a strong impact (Nair et al., 2017). If the radials move out of the high permeable zones, reduction in inflow can be considerable. However, this depends on the relative thickness of the high and low permeability layers and on the question whether all layers are equally jettable. A vertically layered case (the Klaipėda geothermal development) will be investigated in more detail in Chapter 5.

3.3 Impact uncertainty in lateral characteristics

Laterals created using RJD are not steered and don't have a fixed diameter, which makes the characteristics of the created lateral highly uncertain. The uncertainty in the lateral characteristics has two aspects:

- The lateral path and diameter itself are uncertain and are influenced by the subsurface conditions such as fractures or transitions, voids and in situ stress conditions.
- The same deviations from the straight path and predicted diameter have different impact in different geological settings. For example, in thick homogeneous formations, changes in inclination are less likely to change the productivity of a radial than in a thin reservoir, where the laterals could move out of the reservoir.

Below, these two aspects are briefly discussed. The impact of the well and near-well area as characterised by skin is not included, because that is discussed later. In this chapter, mainly a qualitative analyses is presented. In Chapter 5, the overall effect of the uncertainty in the lateral path on injectivity/productivity is quantified in a more structured way via a Monte Carlo approach. At the end of this section a specific aspect of the uncertainty is evaluated namely the impact of curvature of the laterals, which is not handled in Chapter 5.

Influence of subsurface characteristics on the lateral characteristics

Probably the most important aspect of the uncertainty in the lateral path is the lateral length. There are numerous reasons why the design length cannot be reached. Premature stops can occur due to transitions, voids or large open fractures (Protim-Maut et al, 2017; Reinsch et al 2018). Fractures with limited width however can be crossed (Bakker et al., 2019). The impact of shorter than expected laterals is very strong: the increase in productivity depends almost linearly on the length of the lateral (Peters et al., 2015; Nair et al. 2017).

Not only the path of the lateral is influenced by geological settings, also the lateral diameter may differ due to geological conditions. Since the holes are not cased, breakouts can occur and increase the radial diameter (Latham et al., 2019). Thus for less competent rock, a larger diameter can be expected than for more competent rock, both because it is more easily eroded and is more prone to breakouts. For limestones, carbonates or chalk, jetting with acid can create larger diameters (Medetbekova et al., 2018).

Finally, the path of the lateral might be influenced by the in-situ stress conditions. It was observed in a quarry experiment that 4 out of 5 jetted holes changed direction and were finally oriented in the same direction, namely upward (Reinsch et al., 2018). The cause for the change in direction might be the stress condition in the rock, but could also be something entirely different such as the presence of fractures. In laboratory experiments (Bakker et al., 2019) a change in direction as a result of differential stress could not be observed. This might be caused by the fact that the jetted holes were quite short (< 0.30 m). It was observed

DOI: 10.2312/GFZ.4.8.2019.010

however that the rate of penetration (ROP) is higher in the direction of minimum stress (σ_3) than in the direction of maximum stress (σ_1).

Influence of subsurface characteristics on lateral performance

For heterogeneous media, the impact of the uncertainty in the radial path can be much larger. In particular, in thin reservoirs, there is a risk that the radials move out of the reservoir. Also in layered reservoirs, there is a high risk that a part of the lateral is in low-productive layers. This was shown by Nair et al. (2017) for simulation in the Klaipėda reservoir in Lithuania. The authors analysed the impact of uncertainty in kick-off depth, and length, diameter and inclination of the lateral on the productivity of a well with laterals created using RJD. Both changes in inclination and kick-off depth clearly decreased the performance of the laterals (13 and 8 % on average). In Chapter 5, a more complete analysis of the Klaipėda case will be presented.

Curvature

As mentioned, laterals created using RJD are not steered. Instead, the stiffness of the hose under pressure is the only means of keeping the path of the lateral straight (Bakker et al., 2019). This means that the uncertainty in the path is possibly considerable. Currently no observations of paths or diameters from jetted laterals are available in the subsurface. The closest observation of an actual radial path to date are tests from jetting radials in a quarry (Reinsch et al, 2018). These observed paths deviate considerably from a straight line. The curvature as observed in the quarry means that the lateral reaches less far from the well, potentially reducing the benefit of the lateral. To test the effect of curvature, the paths observed in the quarry experiment (Reinsch et al., 2018) were simulated: first for a homogeneous reservoir having an isotropic permeability of 200 mD; second for an anisotropic permeability of 200 mD in horizontal direction and 20 mD in vertical direction. The simulations imposing curved laterals were compared to the simulations with straight laterals having the same length.

For these simulations, the settings as used in Peters et al. (2018) were adopted, which will be described below. The simulations were performed with OpenGeoSys (Watanabe et al., 2017). The first case is a vertical well with a single kickoff with four orthogonal and horizontal laterals in a homogeneous, anisotropic reservoir of 100 m thick (from 2500 to 2600 m depth). The length of the four radials is 5.46 m, 4.59 m, 3.59 m, and 5.25 m, respectively. The initial pressure is 250 bar (at 2500 m depth) with a hydrostatic pressure distribution in the vertical. Horizontal permeability is 200 mD, vertical permeability is 20 mD and porosity is 0.2. The lateral boundary conditions a constant pressure boundary on the edge of the model, which is at 1000 m from the well. Top and bottom of the reservoir are no flow boundaries. The reservoir fluid is water with a salinity of 150.000 ppm, which has, at reference pressure and reservoir temperature, a viscosity of 0.54 cP and density of 1110.2 kg/m^3. The simulations are isothermal. The well is operated as an injector with a fixed injection pressure of 260 bar @ 2500 m depth. Thus, the steady state flow rate for a pressure difference of 10 bar is calculated. The second case considers the same settings as the first case but the measured curvatures of the individual laterals were imposed. The curved laterals are shown in Figure 3-3. The third case is identical with the first case and the fourth case is identical with the second case but both having an isotropic permeability of 200 mD.

The results of the four scenarios are shown in Table 3-1, Figure 3-4 and Figure 3-5. In general, the curvature of the laterals only changes the performance by +/- 10%. For an *anisotropic* reservoir, a performance increase was observed. For an *isotropic* reservoir on the other hand a performance decrease was observed. For an anisotropic medium (Figure 3-5), the curved paths show a higher inflow, because they are oriented more beneficially to the higher horizontal permeability. The isotropic case shows lower inflow performance because the radials reach less far from the backbone.

Table 3-1: Contribution of the radials to the total volume flow considering straight and curved trajectories as measured in field experiments.

		volume flow [m³/d]						
		total	backbone	all radials	radial 1	radial 2	radial 3	radial 4
1st case	RJD straight (anisotropic permeability)	2196.1	2036.9	159.1	48.1	37.2	27.7	46.0
2nd case	RJD measured (anisotropic permeability)	2200.8	2019.2	181.6	49.6	47.4	32.7	51.8
3rd case	RJD straight (isotropic permeability)	2287.0	1975.1	311.9	93.1	74.3	54.6	89.9
4th case	RJD measured (isotropic permeability)	2269.6	1989.7	279.9	78.9	64.3	47.8	88.9

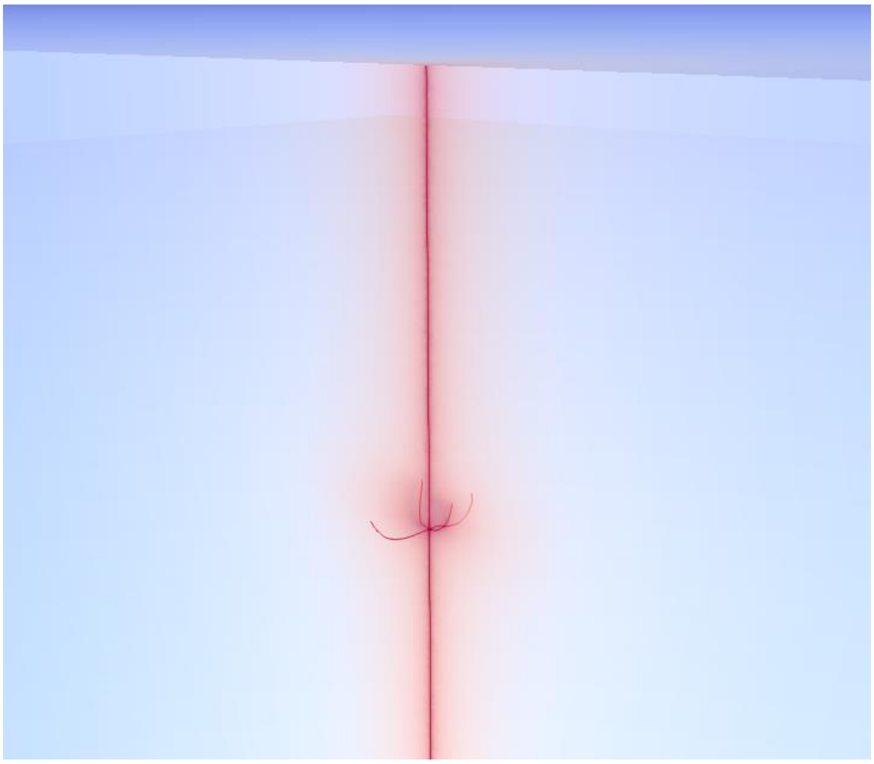

Figure 3-3. Configuration simulated to evaluate the effect of curvature.

DOI: 10.2312/GFZ.4.8.2019.010

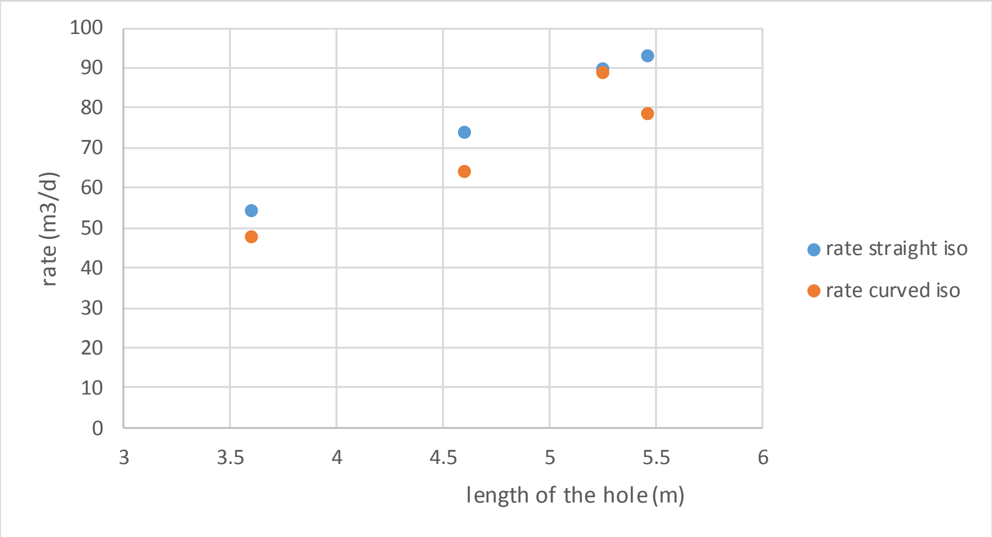

Figure 3-4. Achieved rate for a pressure difference of 10 bar for four radials with different length in case the path is curved and straight for a homogeneous, isotropic medium.

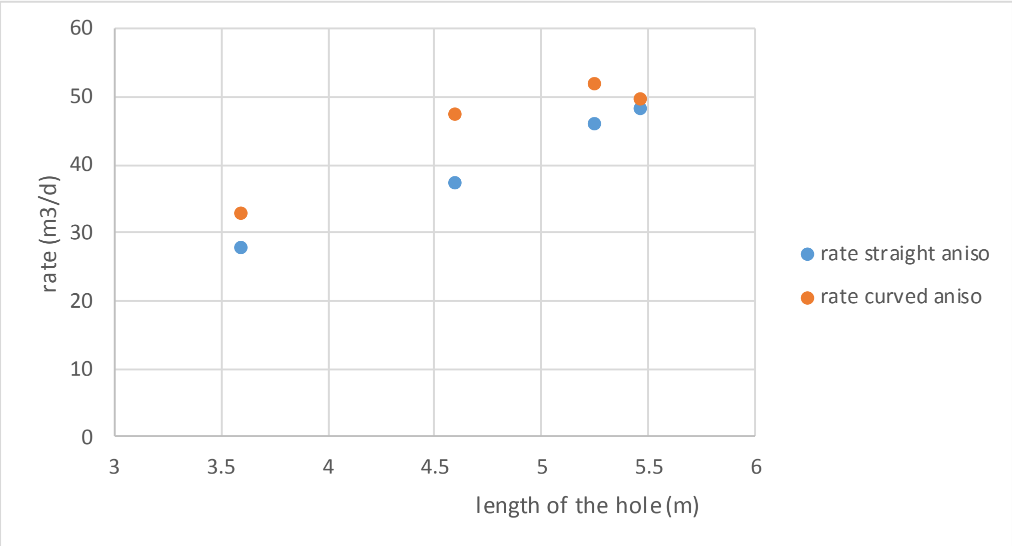

Figure 3-5. Achieved rate for a pressure difference of 10 bar for four radials with different length in case the path is curved and straight for a homogeneous, anisotropic medium.

3.4 Pressure drop

All simulations presented so far have been done by assuming no pressure drop in the entire well. While this is generally a good assumption for the backbone, for the laterals the pressure drop could become important. For the backbone, in general the well diameter is selected to provide minor pressure drop with the design rate. However, radial diameter is less easy to control and not adjusted to the rate. Only the number of laterals can be increased to reduce the rate per lateral. Thus pressure drop might play a role in the design and suitability of radials for

DOI: 10.2312/GFZ.4.8.2019.010

high-rate wells. In this chapter, it will be investigated what the impact of pressure drop in the radials is on the increase of productivity of wells due to radial stimulation.

Pressure drop in open hole can be calculated with the Fanning or Darcy-Weisbach equations. This is an empirical relation that is valid for pressure drop calculations for turbulent flow in pipes. In this equation, the pressure drop depends quadratically on the velocity of the fluid. This in contrast to the Darcy equation for porous media flow in which the pressure depends linearly on the velocity. Including pressure drop in the well makes the solution of the flow problem much harder to solve and more sensitive to time stepping.

For the calculation of the flow with pressure drop in the well, the open source simulator OPM-flow is used (opm-project.org). For the simulation of multi-phase flow in wells, a drift-flux model is used (Bao, 2016), which also includes pressure drop as a result of viscous forces. Since here only single phase flow is used, only the pressure drop calculation is discussed and not the drift flux model. The pressure drop dP due to friction over a length tube L for single phase flow is:

$$dP = 2f\frac{L\rho v^2}{d} \qquad \text{Eq. (1)}$$

where

f : Fanning friction factor

d : tubing inner diameter

ρ : fluid density

v : fluid velocity

The Fanning friction factor is for laminar flow (Re < 2000) is:

$$f = \frac{16}{Re}$$

The Reynolds number Re is defined as:

$$Re = \frac{\rho v d}{\mu}$$

Where μ is the dynamic viscosity. For laminar flow, a no flow condition is assumed on the wall and the pipe roughness does not impact the pressure drop. For turbulent flow the approximation according to Haaland (1983) is used, which relates the Fanning friction factor to the absolute roughness of the tubing. The tubing roughness can be taken as the difference between peaks and valleys on the tubing wall (Bellarby, 2009).

Results

To evaluate the impact of pressure drop in a radial well in geothermal settings, a well with radials is simulated in an infinite reservoir with horizontal permeability of 200 mD and vertical permeability of 20 mD. Grid block size is 10 x 10 x 2.5 m. The well with radials is simulated with and without viscous pressure drop with the settings as listed in Table 3-2. The radials are all 100 m long. In this case, uncertainty of the radial path is not included. Well flow rate, number of radials and radial diameter are varied.

Figure 3-6 shows the change in injectivity with an increasing number of radials without taking into account pressure drop and with pressure drop for two radial diameters (0.04 and 0.05 cm) for a rate of 3600 m^3/d. The figure clearly shows that the increase in productivity of a well stimulated with radials is smaller if the pressure drop is taken into accounted. In Figure 3-7 the injectivity of a vertical well with 4 radials is shown as a function of rate for rates up to 7200 m^3/d. Without pressure drop, the injectivity of the well is independent of the rate and is 322 m^3/d/bar, which is an increase of 57% compared to the well without radials. When pressure drop is accounted for, the increase due to stimulation is only 32 % for a rate of 7200 m^3/d. This impact is considerable and means that for wells with a high flow rate, more radials are required to achieve the same relative increase in permeability.

Table 3-2. Most important settings for the calculation of the pressure drop in the backbone and laterals.

	backbone	laterals
Absolute roughness *e* (m)	0.001	0.01
Diameter *d* (m)	0.25*	0.05

* The diameter of the backbone as used for the inflow calculations was 0.15 m. To avoid pressure drop in the backbone in this sensitivity analysis, the diameter was enlarged for the pressure drop calculations inside the well.

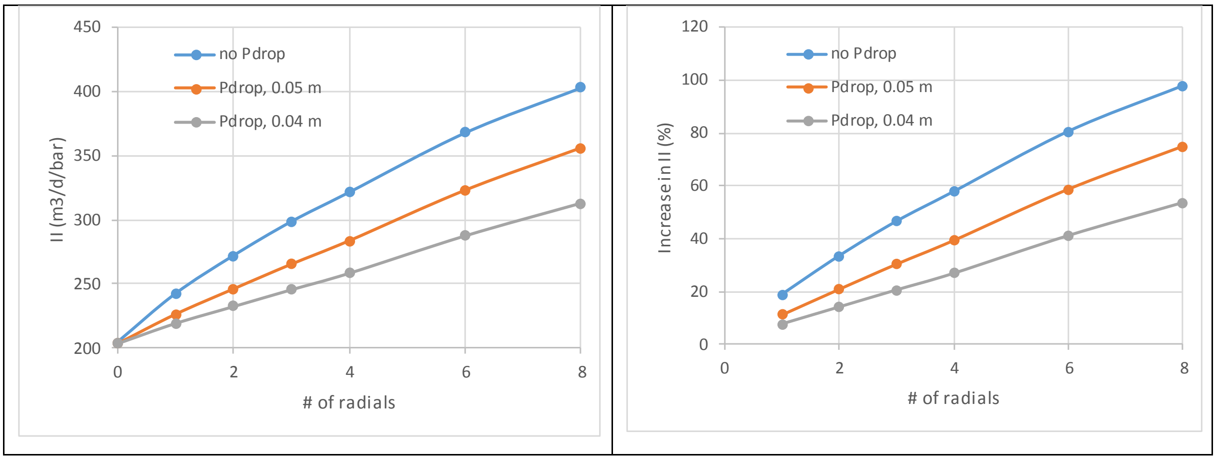

Figure 3-6. Injectivity Index (II) (left) and increase in II (right) as a function of the number of radials without taking into account pressure drop and with pressure drop for two cases of the lateral diameter: 0.04 and 0.05 m.

DOI: 10.2312/GFZ.4.8.2019.010

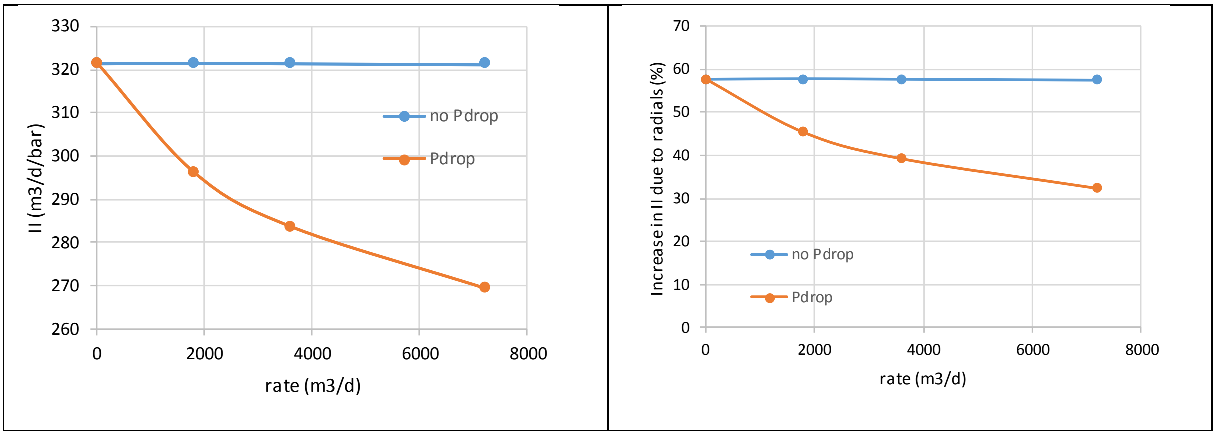

Figure 3-7. Left: Injectivity Index II for a vertical well with 4 radials depending on rate. Without pressure drop, PI is not rate dependent. Right: Increase in Injectivity (%) due to the stimulation with 4 radials as a function of rate (diameter = 0.05 m).

The equations used to calculate the pressure drop are valid for fully-developed, steady-state, incompressible flow in straight pipes or tubes, which is generally a good assumption for straight pipes or tubes. The holes created using radial jetting are probably much rougher and less straight than ordinary tubing, even in the case of corrosion. This means that possibly the equations are used outside of the range of validity. To check this, some numerical simulations were done in which the full Navier-Stokes equations are solved using the software tool GOLEM (Cacace et al., 2017). These simulations are not feasible for a vertical well with radials. Instead they are done for a 10 m long section of radial surrounded by a porous matrix (Figure 3-8) having a permeability of 1 mD and a porosity of 0.2.

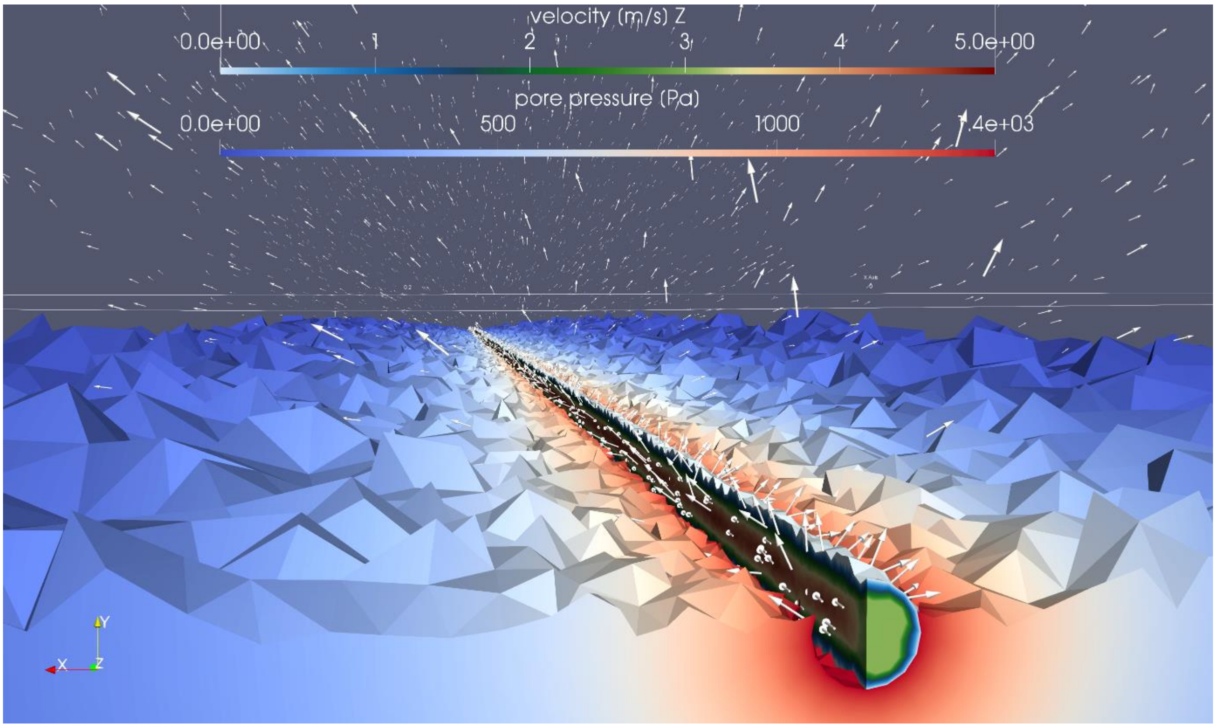

Figure 3-8: Simulated velocity field in the radial in conjunction with the obtained pressure field in the porous matrix.

DOI: 10.2312/GFZ.4.8.2019.010

In order to estimate the total pressure drop in the radial the fluid density and viscosity of the radial must be considered. The dynamic viscosity for all scenarios was set to μ = 4 cP. Furthermore, a surface roughness $\psi = 10.$ which is a random function based on the radius $r = 0.025$ m was imposed:

$$r'(\boldsymbol{X}) = r(\boldsymbol{X}) + r(\boldsymbol{X}) * rand() * \psi/100 \qquad \text{Eq. (2)}$$

Four simulations were performed with an inflow rate of approximately 130 m³/d to analyse the influence of the fluid density on the pressure losses in the radial. The rate of 130 m^3/d is selected, because this is in the range that can be expected under operational conditions. The density was stepwise increased by one order of magnitude from 1 to 1000 kg/m³. Increasing the density will alter the Reynolds number and therefore the flow behaviour (laminar – turbulent) within the radials. As shown in Table 3-3, the flow pattern significantly changes for density above 100 kg/m³ (Re~1000). For such conditions the transition between laminar and turbulent flow occurs. Furthermore, the flow pattern changes from straight lines parallel to the flow direction (density < 100 kg/m³) to a swirl like flow, indicating turbulent flow (density > 100 kg/m³).

Table 3-3: Changes of flow pattern and Reynolds number due to the density of the injected fluid. The view is into the 10 m long radial in direction of the flow.

Density=1 Re=8.86	Density=10 Re=95.5	Density=100 Re=961	Density=1000 Re=9617
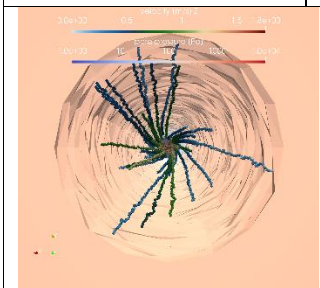	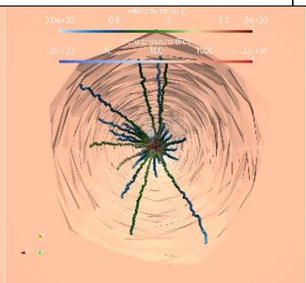	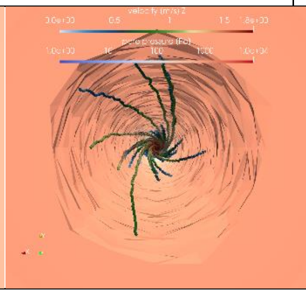	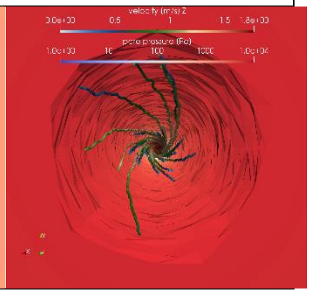

Such a turbulent flow regime will dramatically increase the pressure losses inside the radial. For turbulent flow, the friction loss is found to be roughly proportional to the square of the flow velocity and inversely proportional to the radial diameter, that is, the friction loss follows the phenomenological Darcy–Weisbach equation (Eq. 1). Note that the value of this dimensionless Fanning or Darcy friction factor f depends on the pipe diameter d and the roughness of the pipe surface. In order to validate the Darcy–Weisbach equation for radials surrounded by a porous media, a simulation was performed with increasing inflow rate (0 to 750 m³/d). During this simulation the density was set constant to 1000 kg/m³, the viscosity was 0.4 cP, the radial radius was 0.025 m, and the surface roughness 10% of the radius. The simulated data as shown in Figure 3-9 indicate the non-linear behaviour between fluid velocity and pressure loss. Therefore, these data were used to parameterize the Darcy–Weisbach equation as follows:

DOI: 10.2312/GFZ.4.8.2019.010

$$dP = 2f\frac{L\rho v^2}{d} = 2 * 0.03\frac{10\ [m] * 1000\left[\frac{kg}{m^3}\right] v^2 \left[\frac{m^2}{s^2}\right]}{0.05\ [m]} \quad \text{Eq. (3)}$$

Resulting in a Fanning friction factor of f = 0.03. For comparison, we calculate f using Haalands formula (Haaland, 1983, Eq. 4) in line with the calculations for OPM-flow (opm-project.org) which were done to quantify the pressure drop for a radial well previously:

$$\sqrt{\frac{1}{f}} = -3.6\log_{10}\left(\frac{6.9}{Re} + \left(\frac{e}{3.7d}\right)^{10/9}\right) \quad \text{Eq. (4)}$$

Where e is the absolute roughness in the same unit as diameter d. When using the same input settings as used in the experiment, f is calculated as 0.025, which is in reasonable agreement with the values found in the experiments. In conclusion, under the assumptions used here, the simplified pressure drop calculations using the Darcy-Weisbach formulation in combination with Haalands formulation, appears to be sufficiently accurate to calculation the pressure drop in radials. This enforces the conclusion that the pressure drop in the radials should be taken into account for planning of radial stimulation of a geothermal well.

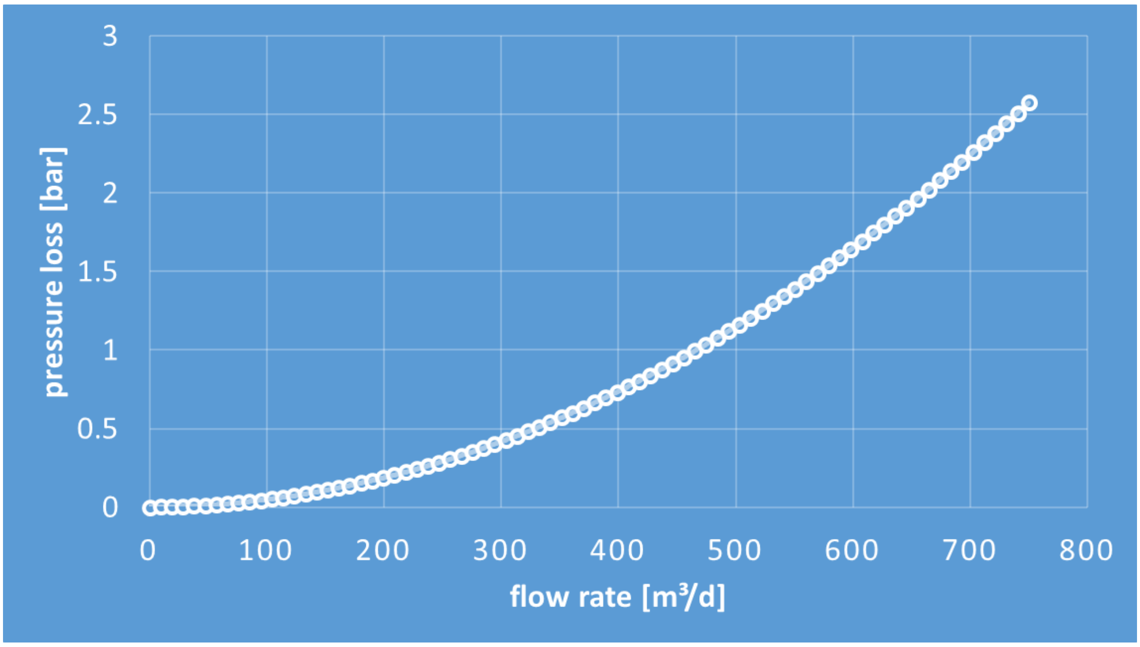

Figure 3-9: Obtained pressure losses for a 10 m long radial surrounded by a porous matrix for increasing injection flow rates.

3.5 Skin and prior well stimulation

The impact of skin on the well to be stimulated is straightforward: in case of positive skin (near-well bore damage), the expected increase due to stimulation with radials becomes larger. For negative skin (the well is already stimulated, for example with a hydraulic fracture), the

DOI: 10.2312/GFZ.4.8.2019.010

expected increase becomes lower. This is illustrated in Figure 3-10, in which the relative increase in well productivity is shown as a function of skin on the backbone. The well configuration is a vertical well (the backbone) which is stimulated with four horizontal laterals and the simulations are done with the semi-analytical tool described in (Peters et al., 2018, 2019).

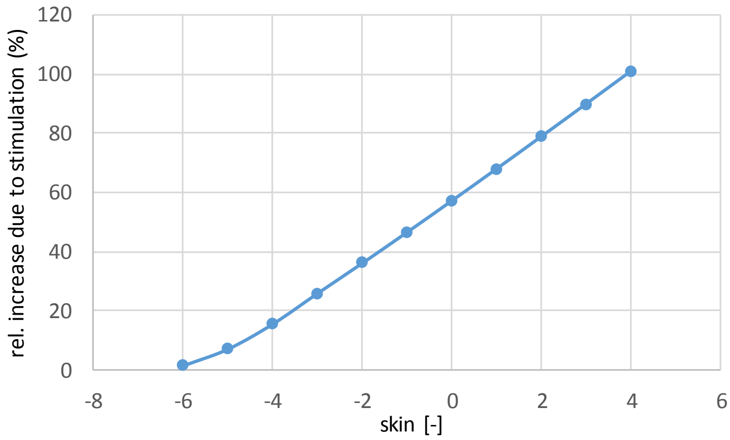

Figure 3-10. Relative increase in production as a function of skin on the backbone as a result of stimulation of a vertical well with four radials.

For very large negative skin (> -5), the impact of adding radials is almost negligible. The reason for this is, that a large negative skin (S) has the same effect as a larger diameter of the well. The relation between an equivalent well bore radius ($r_{w,equi}$) and the original radius ($r_{w,original}$) can be expressed as:

$$r_{w,equi} = r_{w,original} e^{-S} \qquad \text{Eq. (5)}$$

The equation is derived from the steady state analytical solution of inflow into a fully penetrating, vertical well. The 'well' with an equivalent well radius can be visualized as the zone in which no pressure drop occurs. For example, a skin of approximately -7 (for original diameter of the well of 6 to 8 inch) has no pressure drop in a radius of ~100 m around the well. Stimulation with radials cannot move beyond 100 m from the well at the current state of the art and thus cannot enhance such a well, no matter how the skin is caused. For smaller negative skins, details of the skin might have impact on the increase possible due to stimulation.

In the case of naturally fractured reservoirs, most wells have a negative skin in well test interpretation (Slotte and Berg, 2017). This happens because fractures intersect the well and the pressure drop normally resulting from radially convergent flow near the well does not occur, because the flow is in the fractures. Reversely a positive skin might be interpreted when no fractures are intersected. In this case, the increase resulting from stimulation with radials depends on the distribution of the fractures: for a dense fracture network of fine fractures, the radials benefit identically from the fractures and the increase in productivity does not depends much on the skin. For few large fractures, the situation is similar to that of a hydraulically stimulated well and increase from radial stimulation is probably less.

DOI: 10.2312/GFZ.4.8.2019.010

3.6 Lateral stability

A very important assumption made for the semi-analytical calculations is that the laterals are stable. Since the laterals are open hole and often (sub-)horizontal, stability is not guaranteed. The stability of the lateral has a large impact on the performance. If the hole fully collapses, it is unlikely that it will contribute as expected. The impact of borehole breakouts is more difficult to assess. On the one hand, the diameter is enlarged, which is positive for productivity. On the other hand, the debris resulting from the breakout might not be removed from the hole due to the low flow velocity. If the breakout occurs during jetting, it is likely that the hole can be cleaned to some extent otherwise the jetting nozzle would get stuck.

As mentioned in the introduction, several authors mention that friable and/or unconsolidated formations should be avoided because stability of the radials is uncertain (Bruni et al., 2007; Abdel-Ghani et al., 2011; Ragab, 2013; Protim-Maut et al., 2017). Two applications with a depth of more than 3 km were identified (Protim-Maut et al., 2017; Al-Jasmi et al., 2018). Of these, the two deepest as described by Protim-Maut (2017) failed. Possible reasons for failure which were mentioned were a low reservoir pressure and prolonged exposure to jetting fluid. Potential instability of laterals was not discussed. The deep RJD job described by Al-Jasmi et al. (2018) did succeed. Neither publication discussed in-situ stress conditions or mechanical strength of the rock. Also no shallower applications were identified which discussed these topics, except in the case of the RJD job in Klaipėda, Lithuania in which failure of the laterals is mentioned as a possible reason for the disappointing results of the job (Blöcher et al., 2016). No information on the orientation of jetted radials in relation to the main stress directions was found in literature.

Lateral stability was investigated in other tasks of the SURE project, namely experimentally in Task 4.3 (Bakker et al., 2019) and numerically in task 7.2 (Latham et al., 2019). The stress calculations and simulations in (Latham et al., 2019) confirm that for relatively weak rock with an Unconfined Compressive Strength (UCS) of ~50 MPa, the application depth is quite limited. Even for the normal fault regime (which is the most beneficial in terms of stability), failure of at least half the jet-hole wall (taken to mean hole collapse) is expected to occur at depths of around 2 km or deeper (for hydrostatic pressure conditions). Breakout behaviour can already occur at much shallower depth. This appears to support the remarks that in unconsolidated or friable rocks, RJD should not be used, since most applications are deeper than 1500 m. For depths in excess of 3 km, even for more competent rock (UCS = 100 MPa), breakouts and failure can be expected to occur in most in-situ stress conditions (Latham et al., 2019), possibly explaining the lack of success in the deepest wells described by Protim-Maut et al. (2017). These results support the conclusion by Kamel et al. (2017) that candidate selection for RJD should include in-situ stress analysis and rock mechanics as an essential part of the analysis.

The stability discussed so far only relates to stability immediately after jetting. Also the analyses by Latham et al., (2019) does not include time-dependent processes, such as creep or fines migration. Long term monitoring of the radial stimulation job in the Belayim oil field in Egypt showed that after approximately 1 to 1.5 years the achieved improvements were gone (Ragab, 2013). Overall long term performance of radials is still unclear.

DOI: 10.2312/GFZ.4.8.2019.010

4. Doublet performance

The change in injectivity or productivity of a well due to radial stimulation can be linked to the produced power of a geothermal system, either via lowering of the pumping costs or by increasing the flow rate (Peters et al., 2015). Maaijwee (2017) implemented this by assuming a uniform radial stimulation represented by a skin of -6 in the tool DoubletCalc (available on www.NLOG.nl) for four different formations present in the Dutch subsurface. However, two aspects of a geothermal system which have impact on the performance are not included when only changes in productivity/injectivity are included, namely impact of radial stimulation on production temperature and in particular breakthrough of cold water and the impact of a limited field size. Both will be discussed below.

4.1 Production temperature and cold water breakthrough

Placement of the radials can have impact on the production temperature in several ways. If the rate is increased, breakthrough of cold water will be faster. This is not further discussed, because this is an effect of rate rather than the stimulation as such. Secondly, the depth at which the laterals are placed in the producer directly changes the inflow temperature: placing the laterals deeper increases production temperature directly. Thirdly, the placement of the radials in the injector impacts the production temperature indirectly by increased pressure in the zone were the laterals are located which increases the production from this zone. The last two points is mostly relevant when the payzone from which the hot water is produced is thick (e.g. the Californië case discussed in the next chapter in which hot water is produced over a depth interval of more than 500 m thick) or multiple zones are present. Finally, in later time, the location of the radials can influence the cold water breakthrough, because the distance between the producer and injector can be shortened. The last effect depends on both the radial configuration in the injector and producer and the reservoir architecture. In general though, the effect of all three aspects is quite small. In the following a number of examples is presented to illustrate this.

The impact of laterals on the cold water breakthrough was tested using simulations for a doublet in the Klaipėda reservoir, which is a layered reservoir. This case is explained in detail in Chapter 5. Here only the temperature is discussed. In this doublet, radials are implemented in both the injector and producer and the temperature development over time is simulated. The initial production temperature is 39 °C and injection temperature is 11 °C. The doublet distance is approximately 1500 m and both wells are vertical. The radials are distributed over the depth of the well and are oriented in all directions. Please see Chapter 5 for the details of the simulations. To focus on the impact of the laterals, the wells were run on rate constraint. Four scenarios were run with increasing numbers of radials in both the injector and producer. For each scenario with radials, 30 realizations were simulated representing the uncertainty in the radial path (see Chapter 5).

The production temperature over 100 years for all four scenarios is presented in Figure 4-1. For the scenarios with radials the average is presented. The results in Figure 4-1 show that the impact of the laterals on the temperature is very small. The initial difference in temperature due to different distribution of the inflow over depth is larger than the impact on the breakthrough. It should be noted that if the pressure difference over the wells had been kept constant and the rate allowed to change, then the impact of the laterals would have been much larger due to the changes in rate. To check the deviation between individual realizations of

DOI: 10.2312/GFZ.4.8.2019.010

each scenario, the production temperature after 50 years of the individual realizations is presented in Figure 4-2. This confirms the small spread: even over all the realizations, the difference is less than 1 °C.

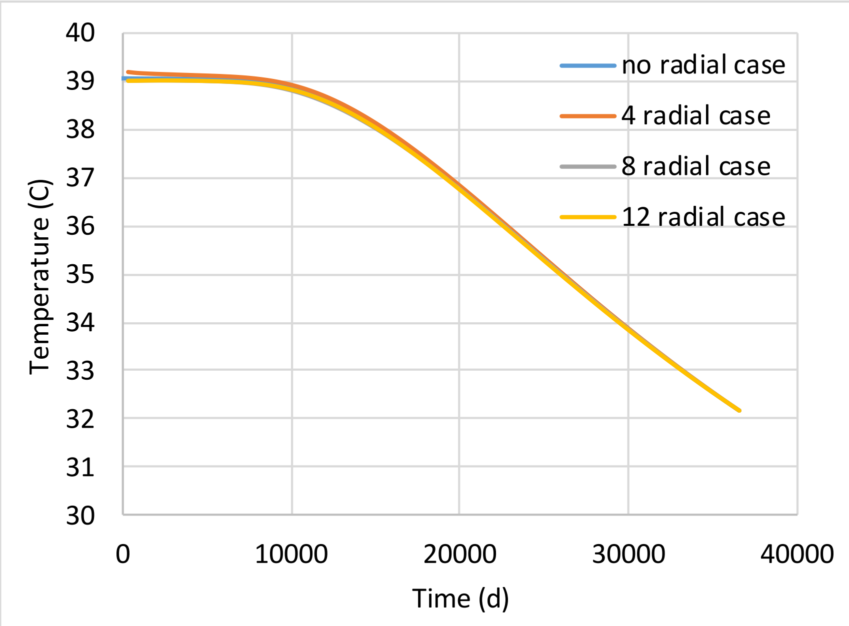

Figure 4-1. Temperature of produced water (°C) over time for 4 scenarios with zero, 4, 8 and 12 radials in both the production and injection well.

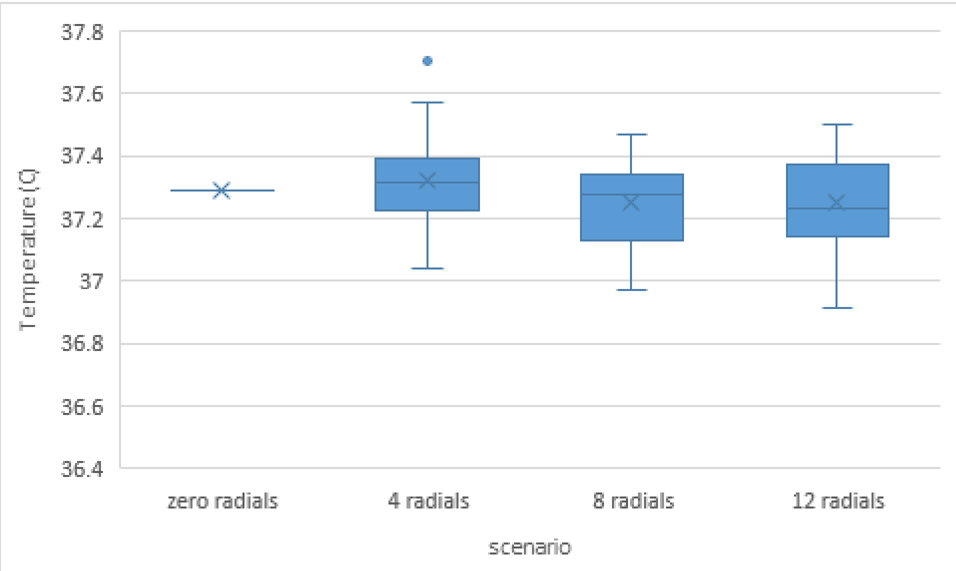

Figure 4-2. Box-Whisker plots of the temperature of produced water (°C) after 50 years for 4 scenarios with zero, 4, 8 and 12 radials in both the production and injection well. (The boxes indicate the quartiles, the lines extending vertically indicates the minimum and maximum (the 'whiskers'), the average is given by a cross and outliers are indicated as dots.)

The second example is in the same reservoir, but focuses on the impact of placing the laterals at a different depth. In this case, 4 radials are placed in producer 2P: once in the top of the

DOI: 10.2312/GFZ.4.8.2019.010

reservoir and once in the bottom. The top part of the reservoir has poorer connectivity between the injector and producer than the bottom part of the reservoir (Figure 5-2). In the injector, the laterals are placed approximately in the middle of the reservoir. The temperature development in Figure 4-3 shows that initially the production temperature is higher due to increased production in the lower part of the well. However, because the good connectivity in the bottom part of the reservoir, the increased production in the bottom increases the flow of cold water in that part. The temperature profile over depth becomes skewed towards the bottom and cold water reaches the producer earlier. The difference after 50 years is still very small at approximately 0.5 °C.

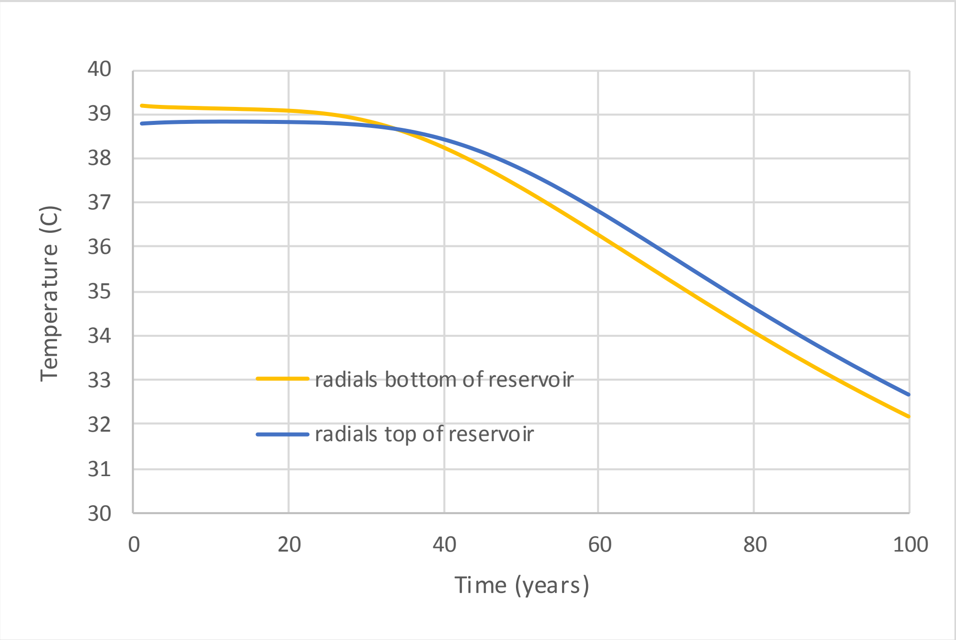

Figure 4-3. Temperature of produced water (°C) over time for different placement of the radials in the producer.

In a third example, the temperature development for the second case study in Chapter 5, Californië is discussed. Again a doublet is analysed, but in this case only in the injector radials are placed, because the performance of the injector is much poorer than of the producer. In Figure 4-4, the temperature in the producer is presented for three different radial configurations with 8, 12 and 16 radials, respectively (see Figure 5-10 for the description of the radial placement). In the 8-radial case, the radials are placed deeper in the reservoir compared to the 12- and 16-radial case. This results in more injection deeper in the reservoir and thus higher production temperature due to the increased pressure support in the deeper part. The radials in the 12- and 16-radial case are more distributed over the entire depth of the injector and show lower production temperature. However, the differences are small in any case (~0.2 °C).

DOI: 10.2312/GFZ.4.8.2019.010

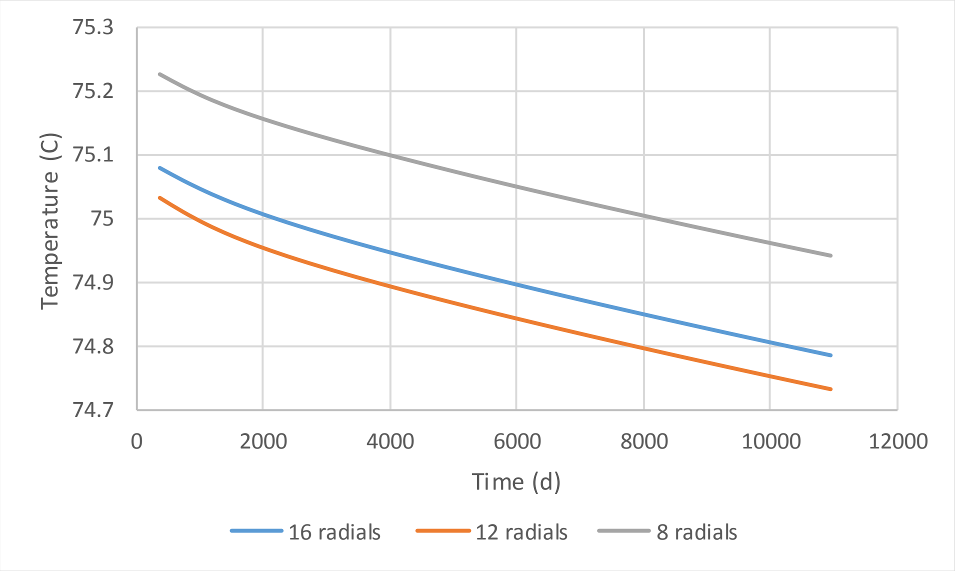

Figure 4-4. Temperature of produced water (°C) over time for different placement of the radials in the injector well.

Salimzadeh et al (2019) analyzed the impact of radials on cold water breakthrough in fractured media. Fracture flow was simulated explicitly via a Discrete Fracture Network rather than a dual porosity approach. The authors analyzed three different fracture densities and different placement of the wells. The temperature decrease in their setup is in the order of 15 to 20 °C from 80 to 60 - 65 °C over a period of 30 years. The authors did not take into account uncertainty in the radial path. The impact of the radials had both negative and positive impact on the cold water breakthrough. In most cases, the speed of the cold water breakthrough was reduced. For the low fracture density with short fractures in which flow is dominated by matrix flow, impact of the radials was very small. For the high fracture density, the impact of the radials was large and was always to reduce the cold water breakthrough. Intermediate density showed intermediate behavior with both positive and negative impact. Only one stochastic realization of the fracture network per case was simulated, which means that different behavior might be found for different realizations.

Including the poro-elastic effects of temperature and pressure on fracture aperture had negligible effect on the cold water breakthrough in this relatively low temperature system (80 °C). The results from Salimzadeh et al (2019) confirmed that for matrix flow, stimulation with laterals has little impact. In low permeability reservoirs where the flow mainly occurs through the fracture network, the RJD laterals should connect to the nearby fracture network in order to be effective.

4.2 Limited field size

If field size is limited, changes in injectivity or productivity of wells alone cannot give the impact on the economic performance of the radial stimulation. This can be seen from the results of a study on radial jet stimulation for gas reservoirs (Abdel-Ghany et al., 2011; Peters, 2015). Both analyse gas production from a gas field of limited size over a fixed period of time. They show that for a gas field of fixed size and a fixed production period, the ultimate recovery benefits more for low permeability than for high permeability. The reason for this is that within the given production period, for high permeability full recovery can already be achieved. The improvement in recovery is the highest for the lowest permeability used (0.001 mD in (Peters, 2015)). However, even though the improvement is good, total recovery is still very low for very low permeability (< 0.01 mD). The benefit of radial stimulation in such a system can also be seen as an acceleration of the production rather than increasing the total that can be produced.

For geothermal systems, such a strongly limited field size is less common. In most geothermal systems, ‘field size’ is determined by the distance between the injector and producer, which determines the timing of the cold water breakthrough and thus the field life. Increasing the rate of the doublet shortens the field life if doublet distance is fixed. In general, radial jet stimulation is used to fix under-performing wells or is planned from the start of a project in which case the doublet distance is adjusted to match the planned rates. In a geothermal system such as an EGS system with a limited stimulated area, the results could be similar to that of a gas field. However, EGS systems are usually in hard rock, which is not jettable with current technology and beyond the scope of this report.

5. Case studies

In this chapter, two detailed case studies with a doublet are discussed. The case studies are based on real field cases. By basing the reservoir models on real field cases, it is ensured that cases are consistent and realistic. To widen the range of applications, variations on the geological base case were created, for example by varying the level of anisotropy or changing the fracture density. For both reservoirs, a sensitivity analysis was performed including the impact of the uncertainty in the lateral path.
The two cases discussed are:

- A doublet in the geothermal reservoir in Klaipėda, Lithuania.
- A doublet in a reservoir based on the geological settings of the Californie area, Netherlands

This work has previously been reported in:
Peters, E., Geel, C.R., Nair, R. and Blöcher, G. Potential of well stimulation using small-diameter laterals in geothermal reservoirs. EGC The Hague, The Netherlands. 2019.

Before discussion of the detailed doublet case studies, a number of single well cases is analysed in which the interplay of well stability, well diameter, pressure drop and heat produced is illustrated. These simulations are done using OPM-flow. The case studies have been simulated using Eclipse 100® with the “temperature option” (Schlumberger, 2016).

5.1 Single well cases

To illustrate the impact of the different aspects such as borehole stability, pressure drop and diameter in relation to the performance, three simple cases were analysed with settings of typical geothermal reservoirs. The approach is very simplified and only serves as illustration. For comparison we will consider three cases:

- Case 1: a weak sandstone with good porosity (0.2) and permeability (200 mD).
- Case 2: a stronger sandstone with poorer porosity (0.1) and permeability (50 mD).
- Case 3: a competent, fractured limestone. Fracture permeability is dominant and the flow is simulated as a single porosity system with a permeability of 100 mD in x- and

DOI: 10.2312/GFZ.4.8.2019.010

z- direction and 10 mD in y-direction caused by orientation of the fractures. Matrix permeability is assumed to be negligible.

In these cases only a single well will be simulated to focus on the changes in potential of the well. Whether this potential is utilized depends on the further geological conditions, such as barriers and boundaries and doublet settings. Realization of full potential also depends strongly on the expected life time of the radials, which at this point in time is still highly uncertain as discussed in Chapter 3 on lateral stability.

To parametrize the cases, it is assumed that for sandstone higher porosity is associated with lower strength of the rock, represented here with Unconfined Compressive Strength (UCS) (Chang et al., 2006) and less stable radials (Table 5-1). The depth at which the, to be stimulated, reservoir is located is based on the depth at which the radials are expected to be stable (without breakouts) irrespective of the orientation of the radial. Stability of the laterals is based on the results presented by Latham et al (2019) assuming normal faulting regime, hydrostatic pressure and estimates of the in-situ stress based on the World Stress Map (Zang et al., 2012). The UCS and depth for Case 1 are taken as 50 MPa and 1 km, for Case 2 it is 100 MPa and 2 km. For Case 3, 150 MPa and 3 km are used.

To estimate reservoir temperature, a thermal gradient of 30 °C/km and average surface temperature of 10 °C are assumed. The reservoir temperature thus becomes 40 °C, 70 °C and 100 °C respectively. The lateral diameter is also adjusted per case. For cases 1 and 3, a larger diameter is used. For Case 1, the diameter is larger because the rock is relatively incompetent (Bakker et al., 2019) and for Case 3, because jetting with acid produces larger diameters (Medetbekova et al., 2018). The lateral length is adjusted for Case 3: due to fractures, it assumed that the likelihood that radials stop prematurely is high: thus 50 m in length (on average) is assumed. Table 5-1 gives an overview of the input settings and results for all cases.

Further input settings are constant for all cases: (net) reservoir thickness is 100 m, pressure drawdown is 20 bar, heat capacity of the brine is taken as 3900 J/kgK. Reservoir temperature is assumed based on a thermal gradient of 30 °C/km. Production temperature is not simulated, but taken the same as the reservoir temperature. The geothermal power produced is calculated by assuming cooling to 20 °C. Transport and cooling in the well to surface are not taken into account. Fluid properties are taken constant with density is 1050 kg/m^3 and viscosity is 0.54 cP. In reality, fluid properties depend on the reservoir temperature and are different for producer and injector due to the difference in temperature. The overall geothermal power of a doublet should take both into account, but this is beyond the scope of this analysis.

Table 5-1. Overview of the main input settings and results for three cases with of stimulation of a vertical well with 4 radials.

	Case 1	Case 2	Case 3
Type	Sandstone	Sandstone	Carbonate

DOI: 10.2312/GFZ.4.8.2019.010

Porosity (-)	0.2	0.1	0.01 (fracture)
Permeability (x,y,z – dir) (m)	200, 200, 20	50, 50, 5	100, 10, 100 (fracture)
UCS (MPa)	~50	~100	~150
Reservoir depth (m)	1000	2000	3000
Lateral diameter (m)	0.05	0.03	0.05
Length of the laterals (m)	100	100	50
Temperature (°C)	40	70	100
Rate (sm^3/d) (@ dP = 20 bar)	5506	1355	1378
PI / II ($sm^3/d/bar$) (for given rate)	275	68	69
Increase due to radials (%)	35	33	88
Geothermal power (kW)	5219	3211	5225
Power from radials (kW)	1355	796	2444

The increase in PI / II due to the radial stimulation is much larger for Case 3 (88%) than for Cases 1 and 2 (35 and 33% respectively). This is partially due to a difference in the orientation of the anisotropy and partially due to pressure drop in the radials. The increase due to radials without pressure drop is 58% for both Case 1 and Case 2 and 101% for Case 3. For Case 1 the increase is lowered due to the high rate which causes much pressure drop in the radials. For case 2 the increase is lowered due to the small diameter of the radials. For Case 3, the stimulation is very beneficial, even for radials of 50 m and impact of pressure drop is quite small. This result partially depends on the choice for skin. Fractured reservoirs often show negative skin, because the pressure drop in fractures is less than for radial, porous flow to the well. In that case, the effect of the stimulation will be less.

The heat produced for Case 1 is high because of the large rate. Due to the much larger rate however, doublet distance needs to be larger if the same time to cold water breakthrough should be achieved as in Case 2. Also pump capacity needs to be larger. For Case 3, due to the high temperature, the produced heat is similar to the heat produced for Case 1. Due to the small porosity and fracture flow, risk of breakthrough of cold water is a much larger. Thus the doublet distance also needs to be larger to avoid these risks.

When not taking into account life time of the radials, the benefits from the radials are highest for Case 3 in which the largest amount of heat is produced by the radials. By far the lowest benefits from radials occur in Case 2.

5.2 Klaipėda

Model description

The Klaipėda geothermal plant is located within the West Lithuanian geothermal anomaly with a relatively high heat flow density of 70-90 mW/m^2. The reservoir is composed of a fine-grained friable sandstone (fine and medium grained) from the Lower Devonian called the Kemeri formation (Šliaupa, 2016). The reservoirs has relatively thin reservoirs layers with high permeability between thicker layers of fine grained material with low permeability. In total four wells were drilled: two injectors and two producers (Figure 5-1) (Brehme et al, 2018). To simplify the simulations and interpretation of the results only two wells were used in this model: 1I and 2P.

DOI: 10.2312/GFZ.4.8.2019.010

Three facies are identified: coarse sand, fine sand and clay. Permeability and porosity are constant per facies (Table 5-2), because it is assumed that the variability between the facies is much larger than the variability within a facies. The vertical distribution of the facies is modelled based on the gamma ray log in both wells. Facies distribution was simulated on a fine grid (20 m x 20 m x 1.3 m) using sequential indicator simulation based on the upscaled facies logs in the wells (see Figure 5-1). Permeability and porosity were implemented in the fine grid and subsequently upscaled to the coarser simulation grid. Flow-based upscaling with harmonic averaging was used for upscaling the permeability (Schlumberger, 2017). The resulting permeability can be seen in Figure 5-2. Further settings and input of the model can be found in Table 5-2. The reason for choosing sequential indicator simulation rather than kriging for generating the facies distribution, is that the goal of this model is not the best representation of this reservoir, but creating a reservoir with realistic heterogeneity.

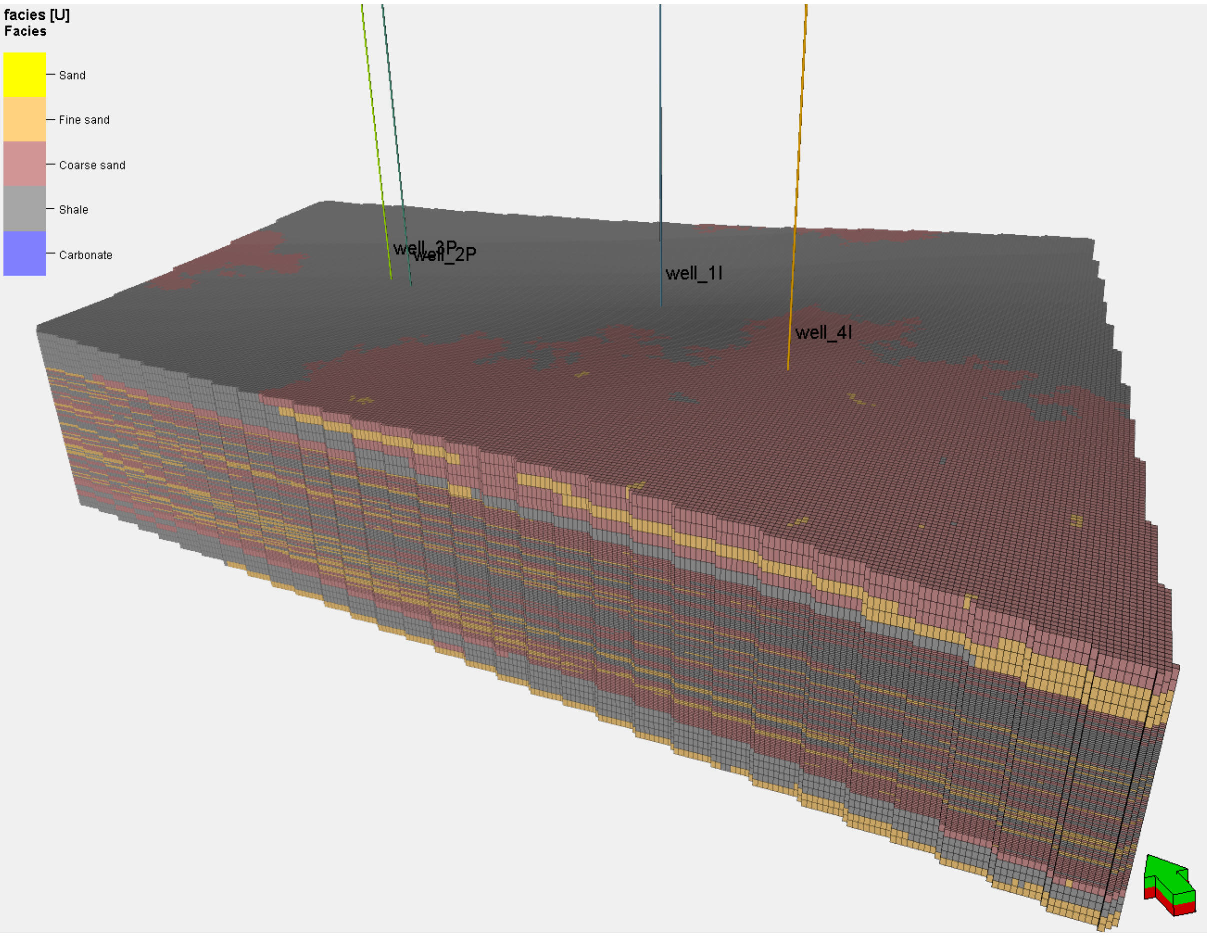

Figure 5-1. 3D representation of the fine grid model, showing the simulated facies property and all 4 wells (vertical exaggeration is 5). Model area is 5400 x 3600 m.

The model is not history matched to observed data, although a check was done to verify that the productivity of the wells was within the range observed in the well tests conducted after completion of the wells. In reality the wells have many issues with decreasing productivity/injectivity over time, in particular the injector (Brehme et al., 2017). This has not been included in this study. Both wells 1I and 2P are vertical and are run on a rate constraint of 9600 sm3/d. Viscous pressure drop in the laterals is not included in the simulations.

Table 5-2. Overview of the Klaipėda model properties

Grid		
Grid Cells (Ni x Nj x NgridLayers)	92 x 114 x 34	
dx x dy x dz	50 m x 50 m x 4.5 m	
Depth interval (approximately)	915 to 1130 m TVDSS	
Rock Properties (fine grid)		
k_h (Coarse sand, fine sand, clay)	1400 mD, 300 mD, 0.005 mD	
Porosity (Coarse sand, fine sand, clay)	0.26, 0.18, 0.05	
Rock compressibility	0.00009 bar^{-1}	
k_v	k_h /10 and k_h /2	
Net/Gross	1	
Thermal Properties		
Thermal conductivity	194 KJ/m/day/K for sand, 161 KJ/m/day/K for clay	
Specific heat capacity (rock, fluid)	2300 kJ/m^3/K, 3.9 kJ/kg/K	
Initial Reservoir Conditions		
Pressure	107.2 bar @ -1047.5 m	
Temperature	39° C @ 1050 m	
Thermal gradient	2 $^\circ$C / 100 m	
Water Properties		
Density @ ref. conditions	1055.4 kg/m^3	
Viscosity	1.42 cP @10 $^\circ$C 0.88 cP @ 38 $^\circ$C 0.51 cP @ 80 $^\circ$C	
Salinity	95 g/l	
Formation Volume Factor	1.0004 rm^3/sm^3	
Compressibility	0.000037 bar^{-1}	
Wells		
	1I	2P
Inclination	90°	90°
Top Perforation	1000.55 m AH	1002.6 m AH
Bottom Perforation	1124.0 m AH	1115.10 m AH
Well diameter	0.31 m	0.24 m

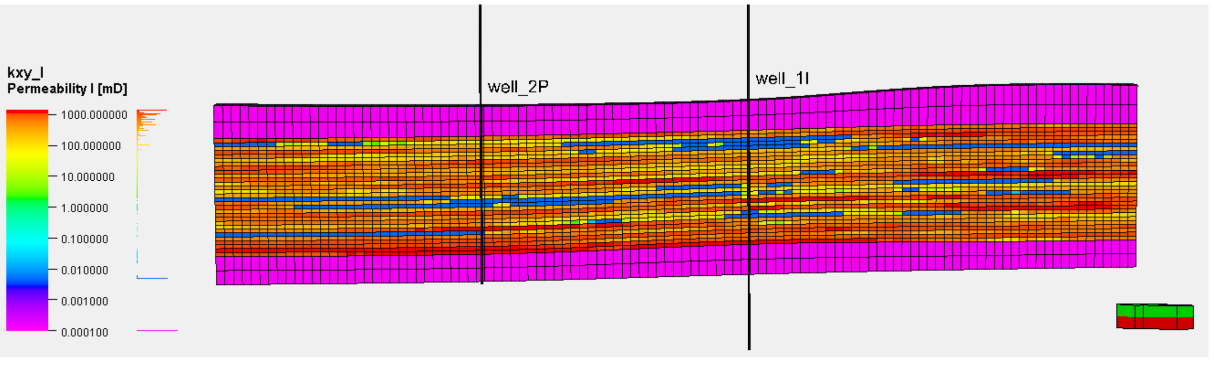

Figure 5-2. Vertical cross-section of the reservoir model showing the horizontal permeability (vertical exaggeration is 5).

DOI: 10.2312/GFZ.4.8.2019.010

Scenarios

Although in reality only well 1I was stimulated with RJD with laterals of length up to 40 m, in this case both wells of the doublet (1I and 2P) will be stimulated and the maximum length is 100 m. Three stimulation scenarios were run: one with 4 laterals, one with 8 laterals and one with 12. The radials are distributed over 4 kickoffs in both wells for the 12-radial case (Figure 5-3). For the cases with fewer radials, kickoffs are removed. For the 8-radial case, the middle kickoff is removed for both 1I and 2P. For the 4 radial case, only the top kickoff is selected.

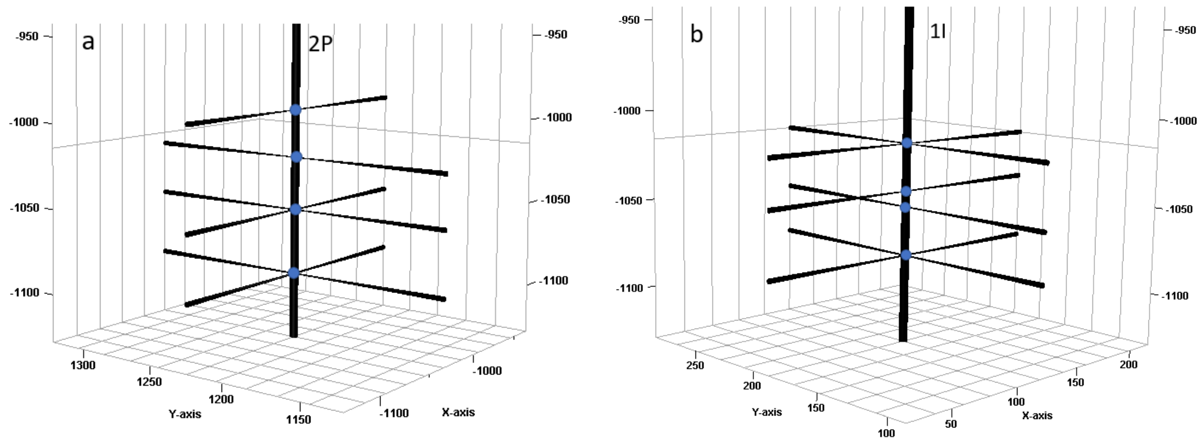

Figure 5-3. Radial well configuration of well 2P (a) and 1I (b) for the 12-radial case.

To account for uncertainty in the radial path, the radial paths were varied. 30 Realizations of the radial paths were made and the resulting flow simulated. The realizations were created by sampling from uniform uncertainty ranges for kickoff depth, length, azimuth inclination and diameter of the laterals. Sampling was done according to a Latin Hypercube scheme. The uncertainty ranges are presented in Table 5-3. Absolute ranges mean that the values used in the simulation are sampled from that range. Relative ranges means that the values sampled from the range are added to the base value, e.g. for the kickoff depth. The minimum value for the length is quite small, because of concerns about the stability of the laterals in the friable Kemeri formation. The range of the radial diameter is quite large, because this includes potential effects of skin and viscous pressure drop due to flow in the lateral. Nair et al (2017) showed that the impact of radial diameter is relatively small. Viscous pressure drop was shown to be important for high flow rates (Chapter 3) and because of the very irregular and rough inner diameter of a lateral compared to normal tubing. Inclination is defined as an absolute range assuming a horizontal base position of the radial.

The representation of the uncertainty in the lateral path is quite simplified here. The laterals are always assumed to be straight and uniform along their entire length. However, representation of these details is not possible with the model approach used here and probably has a smaller effect than the factors included here (see also Chapter 3 on Curvature).

Table 5-3. Uncertainty quantification for the radials.

	Type of uncertainty	Minimum value of the range	Maximum value of the range
Length (m)	Absolute	10	100

DOI: 10.2312/GFZ.4.8.2019.010

Diameter (m)	Absolute	0.001	0.1
Inclination (°)	Absolute	45*	135*
Azimuth (°)	Relative	-90	90
Kickoff point (m)	Relative	-2	2

* 90° is horizontal.

In this analysis we have chosen to analyse the productivity and injectivity of both wells after 10 years for all cases. The reason is that in particular the injectivity declines because of the lower viscosity of the injected, cold water. As the cold water area expands, injectivity declines. This is illustrated in Figure 5-4 below for the case without radials.

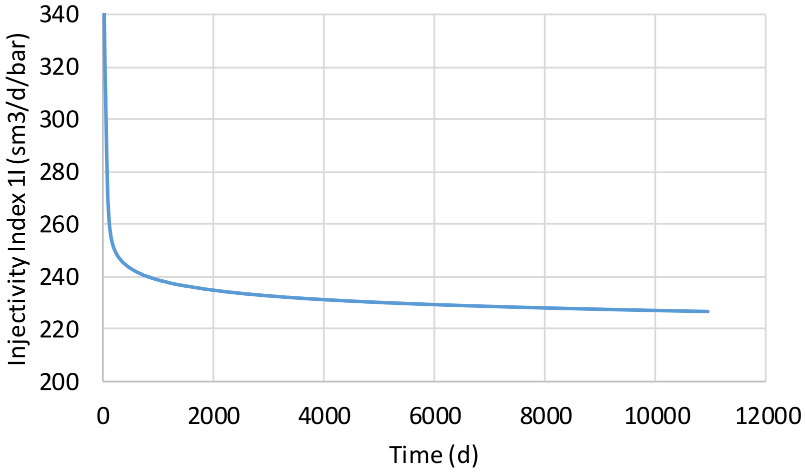

Figure 5-4. Development of the injectivity index of well 1I (sm3/d/bar) over time.

Results

The average increase (from the 30 realizations) as a result of stimulation with 4, 8 or 12 radials is presented in Table 5-4. Two scenarios were analysed: one in which the vertical permeability of 10% of the horizontal permeability and one in which the vertical permeability was 50% of the vertical permeability. In both scenarios, the horizontal and vertical permeability have been applied in the fine grid and subsequently upscaled. This means that the effective ratio horizontal over vertical permeability in the coarser simulation grid can be quite different.

The productivity for well 2P is always higher. For the case without radials this is expected, because the permeability encountered in this well is larger. However, also the increase resulting from radials is larger (Table 5-4). In the analytical modelling (Peters et al., 2015), it was shown that the permeability does not impact the relative increase due to radials. The reason for the larger increase due to radial stimulation is probably due to the larger vertical permeability after upscaling in the area of well 2P.

The increase in vertical permeability shows hardly any effect for well 1I in case of 4 radials (20.0 % versus 23.2%). This is due to the upscaling of the vertical permeability. In the area of the kickoff used in the 4-radial case, upscaled vertical permeability is very small due to the large number of clay layers.

DOI: 10.2312/GFZ.4.8.2019.010

The increase from adding extra radials is not the same going from 4 to 8 and from 8 to 12. This mostly determined by the local permeability in the vicinity if the radials. However, because the increase in injectivity/productivity is calculated for the operating doublet, the wells influence each other. For example, if injectivity improves, the increase in pressure around the well is less, which has a negative impact on the productivity of the producer. For the behaviour of a single well, it is better to analyse the well only. However, in reality wells are run in a doublet setup and therefore this analysis is considered more realistic.

It should be noted that although a sample size of 30 was used, still some difference occurs for different samples. This is however not more than a few %.

Table 5-4. Increase in well productivity/injectivity due to radial stimulation (in %) (average of 30 runs).

	1I		**2P**	
	$k_v = 0.1*k_h$	$k_v = 0.5*k_h$	$k_v = 0.1*k_h$	$k_v = 0.5*k_h$
4 radials	20.0	23.2	29.5	31.5
8 radials	46.9	60.2	59.4	68.0
12 radials	66.5	78.4	71.9	83.3

In Figure 5-5 and Figure 5-6, the results for all simulations are presented in the form of Box-Whisker plots, which also shows the range of the results of the 30 simulations. The uncertainty range is smaller for well 1I and smaller for 4 radials than for 8 or 12 radials. The uncertainty ranges are quite large and overlap for the 8 and 12 radial cases. The discrepancy with the expected increase without including uncertainty is considerable: for example for k_v = 0.1* k_h for 12 perfect radials the expected productivity/injectivity is 474 and 822 sm^3/d/bar for 1I and 2P respectively. From Figure 5-5, it is clear that this is well outside the expected range when including uncertainty. The same is true all the other cases.

This case study shows that generic analysis of improvement resulting from radial stimulation is challenging, due to the variability that can be expected in real cases. Local permeability has a large impact on the actual performance of the laterals. Even if the permeability in the well has been observed, uncertainty is large because the radials move outside of the near-well area.

GFZ German Research Centre for Geosciences
DOI: 10.2312/GFZ.4.8.2019.010

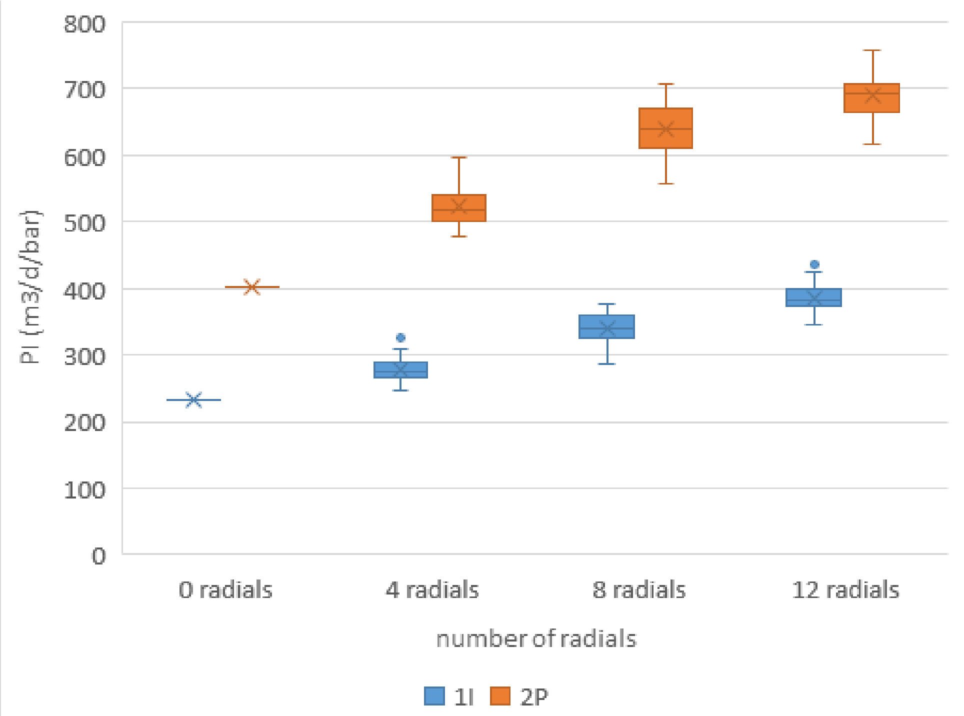

Figure 5-5. Box-Whisker plots of the increase in productivity/injectivity index (PI) for producer 2P and injector 1I for kv/kh = 0.1. (The boxes indicate the quartiles, the lines extending vertically indicates the minimum and maximum (the 'whiskers'), the average is given by a cross and outliers are indicated as dots.)

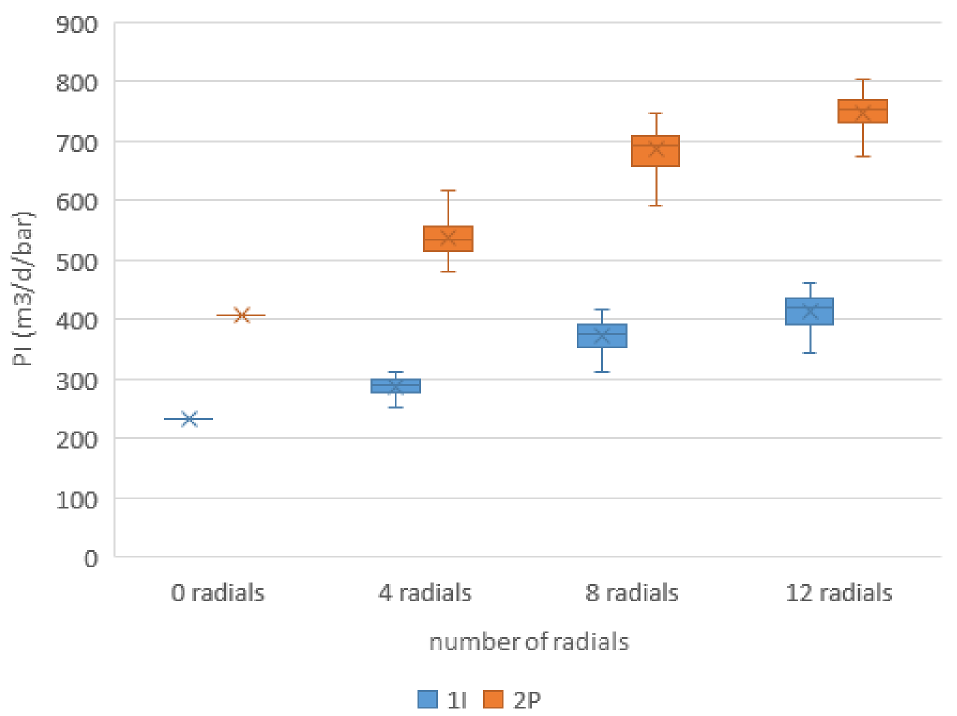

Figure 5-6. Box-Whisker plots of the increase in productivity/injectivity index (PI) for producer 2P and injector 1I for kv/kh = 0.5. (The boxes indicate the quartiles, the lines extending vertically indicates the minimum and maximum (the 'whiskers'), the average is given by a cross and outliers are indicated as dots.)

DOI: 10.2312/GFZ.4.8.2019.010

5.3 Californië

Model description

The Californië geothermal area is located near Venlo in the Netherlands (Figure 5-7). The area contains five geothermal wells: CAL-GT-01 through CAL-GT-05. In this case study, only wells CAL-GT-01 and CAL-GT-02, which are in the public domain are used. The wells have been planned as a doublet, but are currently not in operation. The producer CAL-GT-01 has good productivity and the injector CAL-GT-02 has poor injectivity. The reason for this difference is that the producer is drilled in the direction of a major fault which has a productive fault zone. The injector is drilled away from the fault in an area with much lower permeability. The reservoir section of the wells comprises rocks belonging to four formations (Table 5-5 and Figure 5-8). Since the Californië boreholes penetrated a relatively unknown stratigraphic interval in The Netherlands, it was decided to follow the Belgian nomenclature for the lowermost three stratigraphic units, viz. The Pont d'Arcole Fm, the Bosscheveld Fm, and the Condroz Group.

In the well CAL-GT-01 production stems primarily from limestones belonging to the Zeeland Formation of Early Carboniferous (Dinantian) age. In well CAL-GT-02, the Zeeland Fm is much thinner (~80 m). It is assumed that the flow is distributed over the entire drilled depth, which includes the Devonian rocks of the Bosscheveld Formation and Condroz Group (Table 5-5). All formations have a tight matrix and are dominated by fracture flow. Therefore the area is simulated as a dual porosity medium.

Table 5-5. Reservoir section formations in Californië area

Formation / Group name	Main lithology	Age
Zeeland Fm	limestone	Early Carboniferous (Visean)
Pont d'Arcole Fm	shale	Early Carboniferous (Tournaisian)
Bosscheveld Fm	Dolomites, shales, siltstones, sandstones	Late Devonian to Early Carboniferous (Famennian to Tournaisian)
Condroz Group	sandstone/quartzite	Late Devonian (Famennian)

The thin Pont d'Arcole Formation (Table 5-5) separates the Zeeland Fm from the older siliciclastic rocks. It has not yet officially been described in the Dutch stratigraphy, but is known from Belgium and Germany. It does not contribute to production. Similarly, rocks belonging to the Condroz Group have not been described in the Dutch stratigraphy, but they are known from the Belgian stratigraphy. Rocks of Devonian age have seldomly been drilled in the Netherlands. In Belgium, on the other hand, Devonian rocks are mined at various opencast sites. A transition zone exists between these rocks and the dolomites and limestones of the Zeeland Formation. This zone contains rocks of varying lithological composition that are grouped into the informal Bosscheveld Formation. Rocks of this formation are claystones, limestones and sandstones.

DOI: 10.2312/GFZ.4.8.2019.010

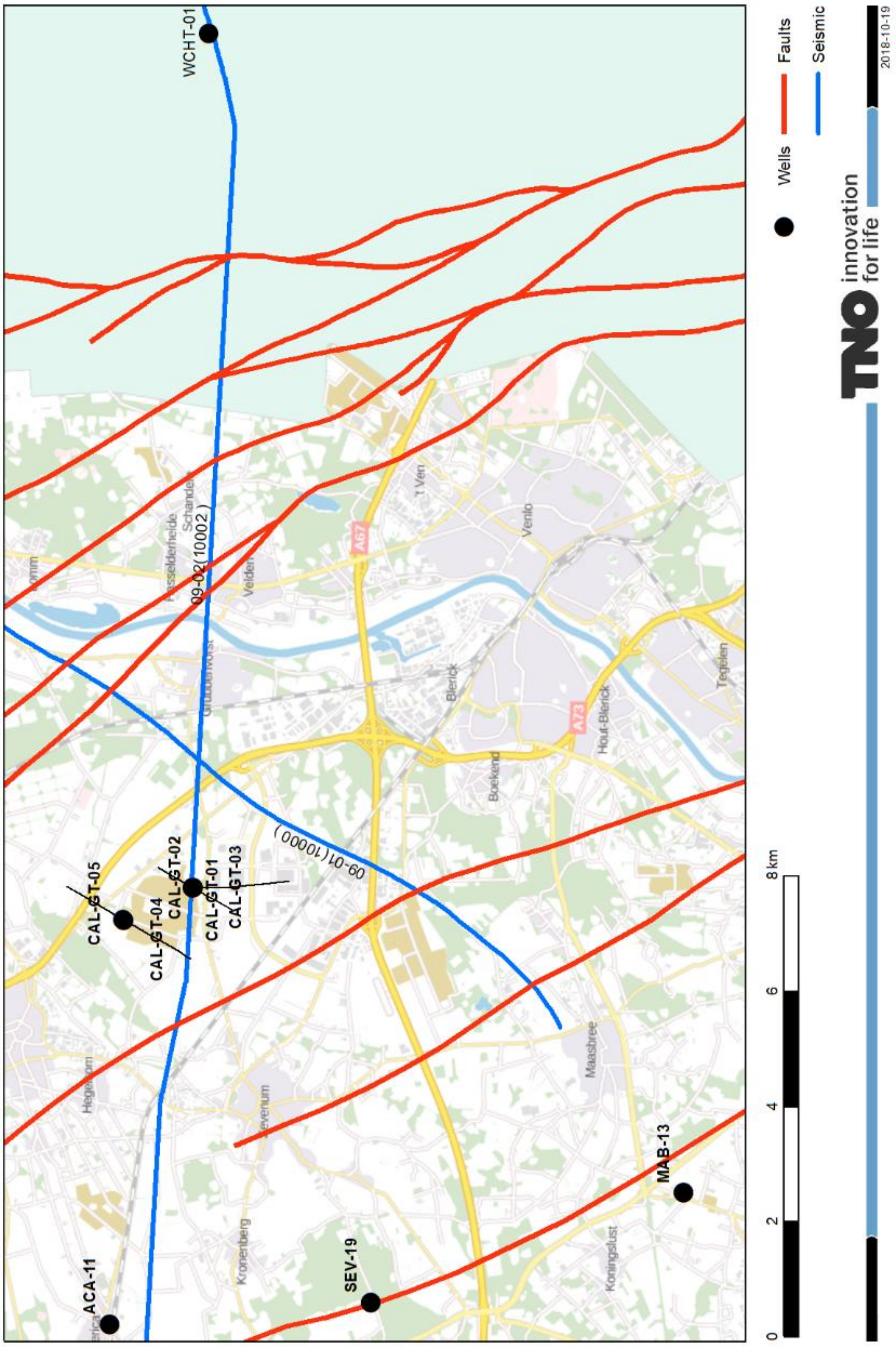

Figure 5-7. Overview of the Californië area. In red are shown the major faults (at surface). In blue, the available seismic lines are indicated. Black dots are well head locations.

DOI: 10.2312/GFZ.4.8.2019.010

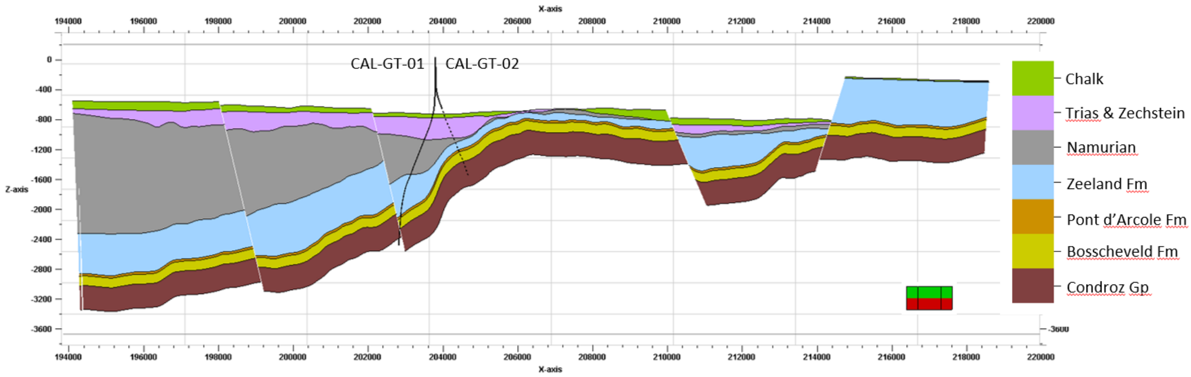

Figure 5-8. Cross section of the Californië area.

A geological model has been created in-house by TNO, and is very similar to the model described in Reith (2018). Because of the complexity of the local geology and the limited availability of seismic data, the model uncertainty is quite high. The goal of the model is not an exact representation of the local situation, but a realistic dual-permeability model with variability in the fracture density. Therefore, the model is not history matched to actual production data.

The main control on the fracture distribution is assumed to be the faults. Around faults, often a damage zone occurs which has increased permeability (e.g. Johri et al. 2013; Bauer et al., 2016) due to fractures. The width of this zone depends amongst others on the history of the fault (especially displacement) and the rock type. Hydrothermal alteration can further impact the permeability of the fractures. It is not known how wide the fault damage zone around the Tegelen fault is. However, from the high injectivity of CAL-GT-01 and CAL-GT-04, it is likely that such a zone exists. For the model, it is assumed that the fracture density depends on the distance to faults (D) and can be calculated as (Figure 5-9):

$$I_{fr} = 0.5D^{-0.8} + 0.5e^{-D^2/(2*220*220)} \qquad \text{Eq. (6)}$$

To account for the orientation of the fractures the fracture permeability is taken anisotropic: the horizontal (along bedding) permeability perpendicular to the fault (j-direction) is taken 100 times smaller than the permeability parallel to the fault (i-direction). The vertical (cross-bedding) permeability is taken as 10 % of the maximum horizontal permeability. In summary:

$$k_{fr,i} = 20I_{fr}$$
$$k_{fr,j} = 2000I_{fr}$$
$$k_{fr,k} = 200I_{fr}$$

Also the fracture porosity and matrix-fracture interaction have been made dependent on the fracture density (Table 5-6). Further input properties are listed in Table 5-6. The Pont d'Arcole Fm is assumed to have zero porosity and permeability.

DOI: 10.2312/GFZ.4.8.2019.010

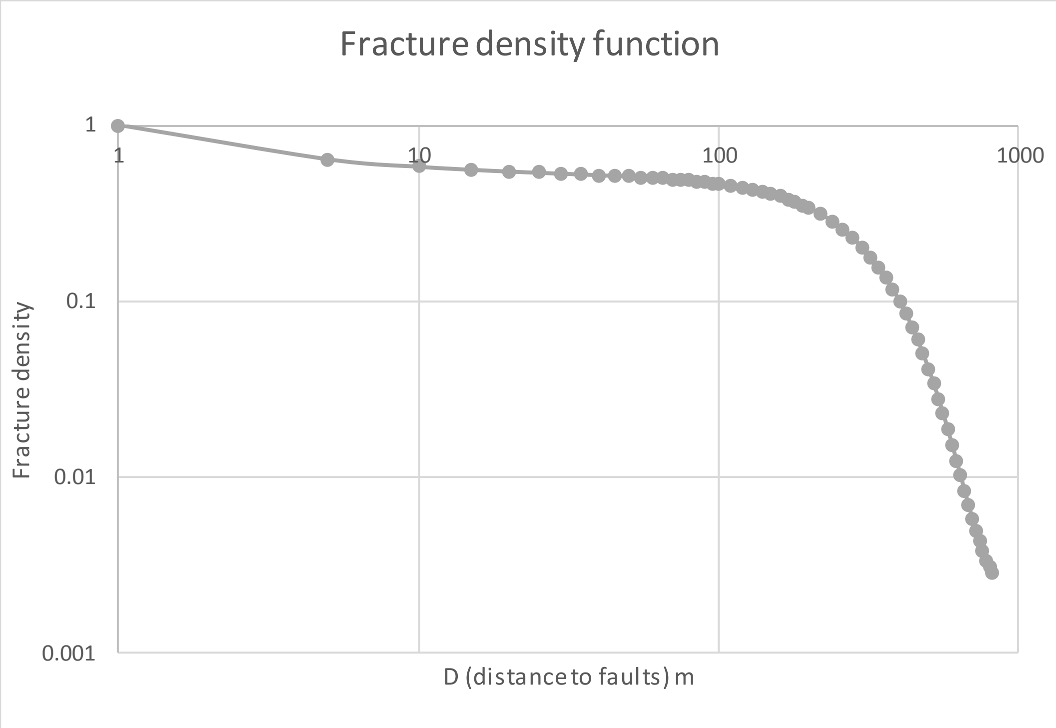

Figure 5-9. Fracture density as a function of distance.

Table 5-6. Overview of the Californië model properties

Grid	
Grid Cells (Ni x Nj x NgridLayers)	185 x 262 x 41
dx x dy x dz	50 x 50 x variable (mostly 10-20 m)
Depth interval (approximately)	1500 – 2500
Rock Properties	
k matrix	10 mD (Zeeland Fm); 0.1 mD (Devonian)
Porosity matrix	0.04 (Zeeland Fm); 0.01 (Devonian)
k fractures	Depends on fracture density (see eq. 6)
Porosity fractures	0.05*I_{fr}
σ_v matrix fracture coupling	12*I_{fr}
Rock compressibility	0.00001 bar^{-1}
Net/Gross	1
Thermal Properties	
Thermal conductivity	224 KJ/m/day/K
Specific heat capacity (rock, fluid)	2700 kJ/m^3/K, 3.7 kJ/kg/K
Initial Reservoir Conditions	
Pressure	105 bar @ 1000 m
Temperature	62.5 ° C @ 1530 m
Thermal gradient	3.423 °C / 100 m
Water Properties	
Density @ ref. conditions	1034 kg/m^3
Viscosity	1.35 cP @10 °C 0.67 cP @ 50 °C

DOI: 10.2312/GFZ.4.8.2019.010

	0.41 cP @ 90 °C	
Salinity	50 g/l	
Formation Volume Factor	1.017 rm^3/sm^3	
Compressibility	0.00004 bar^{-1}	
Wells		
	CAL-GT-01 (producer)	CAL-GT-02 (injector)
Inclination	~35° (reservoir level)	~35° (reservoir level)
Well diameter (bit size)	0.22 m	0.22 m

Both wells are completed as open hole. The wells are run on rate constraint at the relatively modest rate of 2000 sm^3/d, because the injectivity of CAL-GT-02 is too poor to sustain higher rates.

Scenarios

Radials are only placed in well CAL-GT-02, because well CAL-GT-01 already has high productivity. Three scenarios for the radial well design were run: with 8, 12 and 16 radials. The radials are always grouped 4 per kickoff. The kickoffs are distributed over the length of the open hole part, which is 419.2 m. For the case with 12 radials, the kickoffs are shown in Figure 5-10 and are 30, 193 and 343 m AH below the top of the open hole section. For the 8 radial case, the top kickoff point is left out. For the 16 lateral case the kickoff depths are 30, 170, 270 and 370 m AH below the top of the open hole section.

Two scenarios for the permeability were run in order to examine the impact of anisotropy: $k_i = 20 I_{fr}$ (as described in the input) and $k_i = 200 I_{fr}$ (10 times larger).

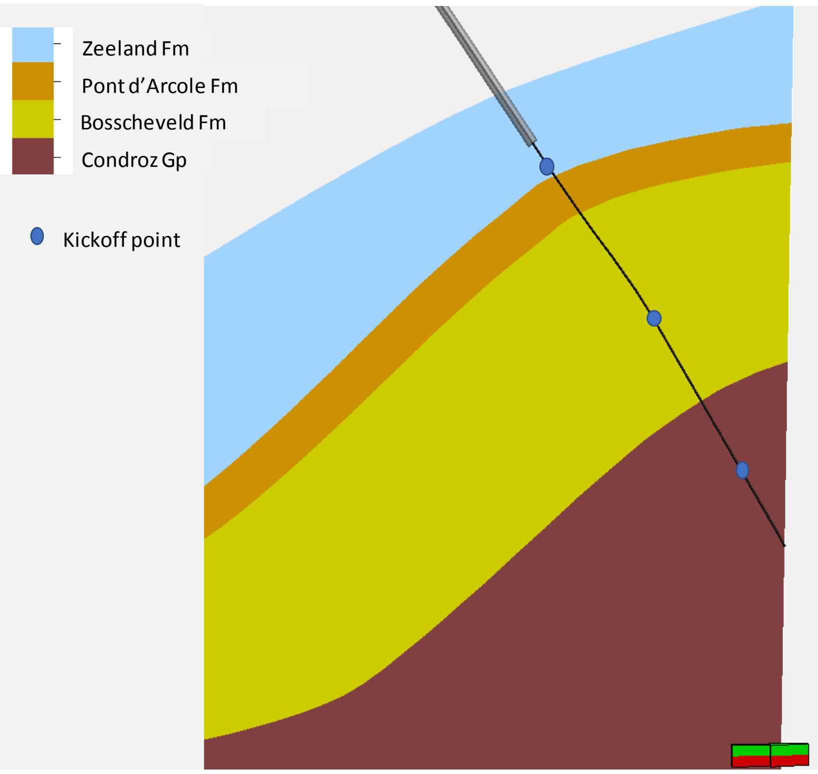

Figure 5-10. Distribution of the kickoff depths in well CAL-GT-02 for the 12 radial case.

DOI: 10.2312/GFZ.4.8.2019.010

The uncertainty quantification is done in the same way as for the Klaipėda case, with the same settings for the uncertainty. Preferably the uncertainty settings should be adjusted to the local conditions. As discussed in Chapter 3, orientation of the laterals to the in-situ stress field is inconclusive. As for the stability of the laterals, for homogeneous rock it is not likely to be an issue since both the rocks from the Zeeland Fm. and Condroz Group are well consolidated, the depth is less than 2500 m and it is a normal faulting regime (Latham et al., 2019). However, heterogeneities such as fractures can cause instability. In two of the five wells in the area, well collapse in the open hole parts of the wells has occurred (Reith, 2018). In addition, when fractures or karst is encountered, premature stop of the jetting can occur.
Therefore, the same settings as for the Klaipėda case were used for the uncertainty. This also facilitates the comparison. The only difference is that 25 instead of 30 realizations of the uncertainty were run, because running this model is much more time consuming.

Results

An overview of the results is presented in Table 5-7, which shows the increase in injectivity of CAL-GT-02. The injectivity of the well was 11.9 sm^3/d/bar without stimulation for $k_i = 20I_{fr}$ and 24.1 sm^3/d/bar for $k_i = 200I_{fr}$. The increase in injectivity for this well is much larger than the increase achieved for Klaipėda, also for the same number of laterals. The reason for this is that the inflow into the radials in Klaipėda was dominated by the lower horizontal permeability, whereas the inflow into the vertical backbone was dominated by the higher horizontal permeability. For CAL-GT-02, both the backbone and the radials are dominated by all three permeabilities, although the backbone benefits more from the increased i-direction permeability than the laterals: the increase for the scenario with $k_i = 200I_{fr}$ is less than for $k_i = 20I_{fr}$.
The impact of the radials on the produced water temperature was examined. Cold water breakthrough doesn't occur in this doublet within 50 years, because of the favorable orientation of the fracture permeability which diverts the cold water away from the production well. The production water temperature is influenced by the placement of the radials: deeper radials increase the pressure in deeper layers and thus increase the temperature of the produced water.

Table 5-7. Increase in well injectivity due to radial stimulation (in %) (average of 25 runs).

	CAL-GT-02	
	$k_i = 20I_{fr}$	$k_i = 200I_{fr}$
8 radials	68.2	43.5
12 radials	126.3	77.2
16 radials	162.0	98.5

In Figure 5-11 and Figure 5-12 the injectivity index II is presented for all scenarios. The uncertainty ranges from the cases with 8 and 12 radials are similar to Klaipėda. For the 16-radial case the uncertainty range becomes larger and shows much overlap with the 12-radial case. Just as for the Klaipėda case, the increase in injectivity calculated for perfect radials without uncertainty is much larger: for example for $k_i = 20I_{fr}$ and 12 radials the simulated injectivity is 47 sm^3/d/bar which is higher even than the maximum for 16 radials.

It should be noted that due to the coarseness of the grid, the numerical error of the simulation of the radials is probably quite large (Peters et al., 2018). However, this is not likely to change the overall results.

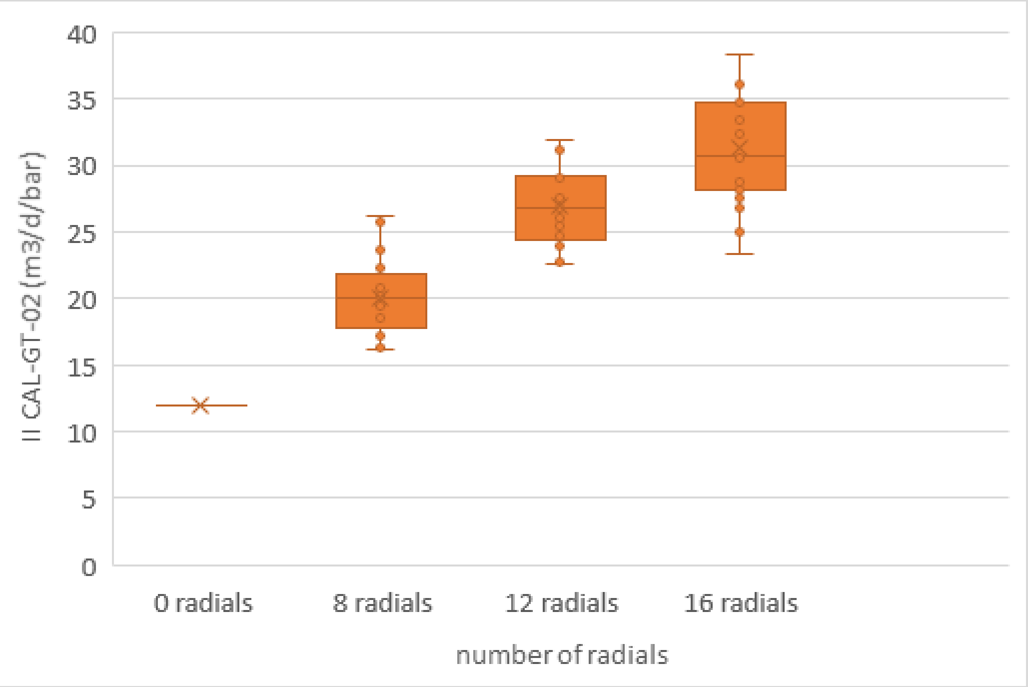

Figure 5-11. Box-Whisker plots of the injectivity index (II) for CAL-GT-02 for $k_i = 20I_{fr}$*. (The boxes indicate the quartiles, the lines extending vertically indicate the minimum and maximum (the 'whiskers'), the average is given by a cross and outliers are indicated as dots.)*

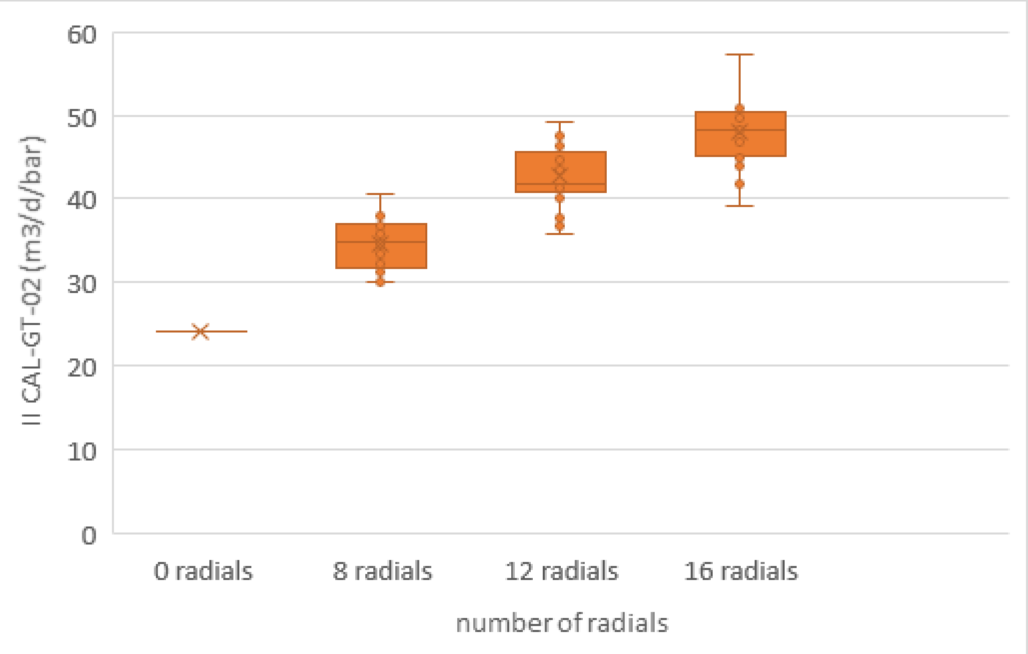

Figure 5-12. Box-Whisker plots of the injectivity index (II) for CAL-GT-02 for $k_i = 200I_{fr}$*. (The boxes indicate the quartiles, the lines extending vertically indicate the minimum and maximum (the 'whiskers'), the average is given by a cross and outliers are indicated as dots.)*

DOI: 10.2312/GFZ.4.8.2019.010

6. Summary and conclusions

In this report, the performance of radials for different subsurface conditions has been analysed. It is clear that the potential for radial stimulation is good: in many subsurface conditions a clear increase in the injectivity or productivity can likely be achieved (in the range 10 to 100% for most cases in this report). The analysis has shown that many aspects influence the expected performance of the radials and that there is no straightforward answer under which subsurface conditions radials are most beneficial. Important aspects to consider are:

- Depth, in-situ stress conditions and formation strength of the reservoir to be stimulated: for applications in weak or friable formations or deep applications estimates of the expected stability of radials at the intended depth are essential.
- Orientation and anisotropy of the permeability: in case the backbone is not orientated optimally compared to the permeability, stimulation with radials is more beneficial because they can take advantage of the higher permeability in other directions.
- Expected rates: high rates require more radials due to increasing frictional pressure drop in the radials
- Heterogeneity of the permeability: highly layered systems and high heterogeneity makes the expected benefits and jettability more uncertain
- Thickness of the reservoir: thicker reservoirs require more radials
- Presence of fractures: in fractured reservoirs, many aspects of the radials are more uncertain, such as jettability, length of the laterals, connectivity to the reservoir and potential impact on cold water breakthrough. The range in expected benefits is larger and more uncertain. The same is true in case of karst.
- Presence of skin: near-well damage (positive skin) increases the expected benefits, prior stimulation of the well (negative skin) decreases expected benefits.

Of course, in addition, all aspects that are normally analysed for drilling jobs, such as for example the well completion, presence of (swelling) clays and fines migration, should also be evaluated.

Important aspects to include when simulating the expected benefits of radials are:

- Uncertainty in the radial path and diameter
- Pressure drop in the radials
- Presence of skin
- Size of the reservoir: for small reservoirs/field size the laterals accelerate the production rather than increasing the total produced volume (oil, gas or heat).

The first two aspects can reduce the expected benefits from radial stimulation considerably. Presence of a positive skin increase the expected benefits, whereas prior stimulation (negative skin) decreases expected benefits. The impact of radials on cold water breakthrough appears to be minor in most cases. Only in fractured reservoirs this might be important.

From the detailed cases discussed in this paper, it is clear that predictions of expected increase due to radials are inherently highly uncertain because of the uncertainty in the radial path and because of the dependence on the detailed permeability distribution around the well. The results shown here confirm the conclusion by Nair et al (2017) that not taking into account the

DOI: 10.2312/GFZ.4.8.2019.010

uncertainty in the radial path results in overestimation of the expected increase in production. The results confirm what was observed in field cases (Peters et al., 2015) that wells with positive skin are good potential targets for lateral stimulation, whereas a large negative skin will reduce potential benefits.

7. Acknowledgements

The SURE project has received funding from the European Union's Horizon 2020 research and innovation programme under grant agreement No 654662. The content of this presentation reflects only the authors' view. The Innovation and Networks Executive Agency (INEA) is not responsible for any use that may be made of the information it contains. The use of data from the Klaipėda site received from Geoterma and from the Californië site from Pieter Wijnen (via NLOG.nl) is gratefully acknowledged. The use of open source codes Field-Opt by NTNU and OPM-flow (https://opm-project.org/) is gratefully acknowledged.

8. References

Abdel-Ghany, M.A., Siso, S., Hassan, A.M., Pastura, P., and Cherri, R. (2011). New technology application, radial drilling, Petrobel, first well in Egypt. In Offshore Mediterranean Conference and Exhibition, 23-25 March, Ravenna, Italy, number OMC-2011-163.

Al-Jasmi,A.Kh., Alsabee, A., Al-Awad, A., Attia, A. and Elsayed, A. (2018) Improving well productivity in North Kuwait well by optimizing radial drilling procedures. SPE-188516-MS.

Bakker, R.R., Simon Hahn, Marc Friebel, David F. Bruhn, Reinsch, T. and Barnhoorn, A. (2019). A laboratory study on radial jet drilling in true triaxial stress conditions. Submitted to Geoscience Frontiers.

Balch, R. (2014). Simulation report - field testing and diagnostics of radial-jet well stimulation for enhanced oil recovery from marginal reserves. RPSEA Project Report.

Bao, K. (2016). Multi-segment wells and well modeling. OPM meeting, Oslo, 1 June 2016. https://opm-project.org/wp-content/uploads/2016/06/opm2016-bao-multi-segment-wells.pdf

Batzle, M. and Z. Wang (1992). Seismic properties of pore fluids. *Geophysics*, 57(11), 1396-1408.

Bauer H. & T. C. Schröckenfuchs & K. Decker. (2016) Hydrogeological properties of fault zones in a karstified carbonate aquifer (Northern Calcareous Alps, Austria). *Hydrogeol J* (2016) 24:1147–1170. DOI 10.1007/s10040-016-1388-9.

Bellarby, J. (2009) Well completion design. Developments in Petroleum Science vol. 56. Elsevier, Amsterdam, The Netherlands.

Blöcher, G. Peters, E. Reinsch, T., Petrauskas, S. Valickas, R. Berg, S. van den. (2016) D3.2 Report on radial jet-drilling (RJD) stimulation technology. SURE report D3.2.

Brehme, M., Blöcher, G., Regenspurg, S., Milsch, H., Petrauskas, S., Valickas, R., Wolfgramm, M. and Huenges, E. (2017) Approach to develop a soft stimulation concept to overcome formation damage – A case study at Klaipeda, Lithuania. PROCEEDINGS, 42nd Workshop on Geothermal Reservoir Engineering, Stanford University, Stanford, California.

DOI: 10.2312/GFZ.4.8.2019.010

Brehme, M., Regenspurg, S., Leary, P. et al. (2018) Injection-Triggered Occlusion of Flow Pathways in Geothermal Operations, *Geofluids*, vol. 2018, Article ID 4694829, 14 p. https://doi.org/10.1155/2018/4694829.

Cacace, M. and Jacquey, A. B. (2017) Flexible parallel implicit modelling of coupled thermal–hydraulic–mechanical processes in fractured rocks *Solid Earth*, 8, 921-941, https://doi.org/10.5194/se-8-921-2017.

Chang, C., Zoback, M.D., Khaksar, A. (2006) Empirical relations between rock strength and physical properties in sedimentary rocks. *J. of Petroleum Science and Eng.* 51, p223–237. doi:10.1016/j.petrol.2006.01.003

Haaland, S.E. (1983) Simple and explicit formulas for the friction factor in turbulent pipe flow Transactions of the ASME, *J. of Fluids Engineering*, 105, No. 1, 89-90.

Hahn, S., V. Wittig, S. Jasper, D. Schwarz, D. Albadroui, K. Hoogland, R.R. Bakker (2019) Deliverable 5.2: Report on Jet drilling at simulated reservoir conditions. Potsdam: GFZ German Research Centre for Geosciences. doi:10.2312/gfz.4.8.2019.002.

Ibeh, S., B. Obah and S. Chiueze (2017) Investigating the application of radial drilling technique for improved recovery in mature Niger Delta oil fields. SPE-189137-MS.

Johri, M., Zoback, M., Dunham, E.M. and Hennings, P. (2013) Fault Damage Zones-Observations, Dynamic Rupture Modeling and Implications on Fluid Flow. AAPG Search and Discovery Article #41249.

Kamel, A.H. 2017. A technical review of radial jet drilling. (2017) *J. of Petroleum and Gas Eng*. 8(8), 79-89. DOI: 10.5897/JPGE2017.0275

Latham, J.P. and A. Farsi, (2019). Deliverable 7.2 - Report on Laterals Stability Modelling.

Maaijwee, C. (2018). InImpact Kennisagenda Radial Jetting, G1345. Panterra GeoConsultants report. https://www.kasalsenergiebron.nl/content/user_upload/G1345_InImpact_report.pdf.

Medetbekova, M.K., S. Salimzadeh, H.F. Christensen, H.M. Nick, (2018) Experimental and numerical study of the stability of radially jet drilled laterals in chalk reservoirs, in: 80th EAGE Conference and Exhibition 2018, Copenhagen, 2018.

Nair, R. Peters, E., Šliaupa, S., Valickas, R., Petrauskas, S. (2017) A case study of radial jetting technology for enhancing geothermal energy systems at Klaipėda geothermal demonstration plant. PROCEEDINGS, 42nd Workshop on Geothermal Reservoir Engineering, Stanford University, Stanford, California, 2017.

Peters, S.A. (2015). Production Performance of Radial Jet Drilled Laterals in Tight Gas Reservoirs in the Netherlands. A Simulation Approach and Economic Analysis. Msc Thesis TUDelft.

Peters, E., Veldkamp, J.G., Pluymaekers, M.P.D. and Wilschut, F. (2015) Radial jet drilling for Dutch geothermal applications. TNO 2015 R10799. Available via http://publications.tno.nl/publication/34620510/4C8joC/TNO-2015-R10799.pdf

E. Peters, J.G. Veldkamp, M.P.D. Pluymaekers and F. Wilschut (2016) Radial jet drilling for Dutch geothermal applications. EGC2016 Strasbourg, 19-24 Sept. Proceedings EGC 2016.

Peters, E. Guido Blöcher, Saeed Salimzadeh, Paul J.P. Egberts, Mauro Cacace. (2018) Modelling of multi-lateral well geometries for geothermal applications. Adv. Geosci. 45, 209-215. https://doi.org/10.5194/adgeo-45-209-2018.

Peters, E., Egberts, P., Chitu, A., Nair, R., Salimzadeh, S., Blöcher, G. and Cacace, M. (2019) The Horizon 2020 SURE Project: Deliverable 7.4 - Upscaling of RJD for incorporation in reservoir simulators, 2019, Potsdam : GFZ German Research Centre for Geosciences, DOI: 10.2312/gfz.4.8.2019.003.

ProtimMaut, P., Jain, D., Mohan, R., Talukdar, D., Baruah, T., Sharma, P. and Verma, S. (2017) Production enhancement in mature field of Assam Arakan Basin by radial jet drilling – A case study. SPE-189243-MS.

Ragab, S. A. M. (2013). Improving well productivity in an Egyptian oil field using radial drilling technique. *Journal of Petroleum and Gas Engineering*, 4(5):103-117.

Reinsch, T., Paap, B., Hahn, S., Wittig, V. and van den Berg, S. (2018) Insights Into the Radial Water Jet Drilling Technology - Application in a Quarry. Doi: 10.1016/j.jrmge.2018.02.001.

Reith, D.F.H. (2018) Dynamic simulation of a geothermal reservoir. Case study of the Dinantian carbonates in the Californië geothermal wells, Limburg, NL. Msc thesis TUDelft (public version).

Salimzadeh, S., Grandahl M., Medetbekova M., Nick, H.M. (2019) A novel radial jet drilling stimulation technique for enhancing heat recovery from fractured geothermal reservoirs. Renewable Energy 139, p395-409. https://doi.org/10.1016/j.renene.2019.02.073.

Schlumberger, (2017) Petrel® User Manual v2017.2.

Schlumberger, (2016) Eclipse® Reference Manual v2016.2.

Šliaupa, S. (2016) Reservoir characterisation of the Klaipėda geothermal plant (Lithuania), Vilnius, Lithuania. Nature Research Centre report.

Slotte, P.A. and Berg, C.F. (2017). Lecture notes in well-testing. NTNU course material TPG4115.

Wang, B., Li, G., Huang, Z., Li, J., Zheng, D., and Li, H. (2016). Hydraulics calculations and field application of radial jet drilling. SPE Drilling & Completion vol. 3, (SPE-179729-PA).

Watanabe, N., Blöcher, G., Cacace, M., Held, S., Kohl, T., (2017) Geoenergy modeling III : enhanced geothermal systems. SpringerBriefs in Energy, Springer, Cham, XII, 104 pp.

Yan, J., Cui, M., He, A., Jiang, W. and Liang, C. (2018). Study and Application of Hydraulic Jet Radial Drilling in Carbonate Reservoirs. *International Journal of Oil, Gas and Coal Engineering*. Vol. 6, No. 5, (2018), pp. 96-101. DOI: 10.11648/j.ogce.20180605.13.

Zang, A., Stephansson, O. Heidback, O. and Janouschkowetz, S. (2012). World Stress Map Database as a Resource for Rock Mechanics and Rock Engineering. *Geotech Geol Eng* 30:625–646.